

11. Quarterly Report 1

3 PLANETARY SOLAR ARRAY DEVELOPMENT 4

Prepared for

14 Jet Propulsion Laboratory  
California Institute of Technology  
4800 Oak Grove Drive  
Pasadena, California 91103  
Attention: G. J. Taix

25 Contract 952035 2500

250 EOS Report 7254-Q-1

13 October 1967 11 /

**R. WIZENICK**

6 Prepared by  
R. Wizenick  
Program Manager

Approved by

**W. Menetrey**

W. Menetrey, Manager  
Power Systems Division

This work was performed for the Jet Propulsion Laboratory, California Institute of Technology, as sponsored by the National Aeronautics and Space Administration under Contract NAS7-100. 25a



**ELECTRO - OPTICAL SYSTEMS, INC.** 10  
A XEROX COMPANY

## ABSTRACT

This report describes the work completed and in progress at EOS during the first quarter of the Planetary Solar Array Development Study Program, JPE Contract 952035.

The report finalizes the requirements of Task I, the environmental definitions of the Martian surface, and gives a preliminary review of the possible concepts as defined in Task II of the program outline.

## CONTENTS

1.	INTRODUCTION	1
2.	TASK I SUMMARY	2
2.1	Martian Environmental Model	2
2.1.1	Mars Atmosphere	2
2.1.2	Thermal Environment	5
2.1.3	Clouds and Dust	5
2.1.4	Solar Intensity	8
2.1.5	Radiation Environment	10
2.1.6	Summary of Mars Probable Environmental Model	10
2.2	Mission Restraints	13
2.2.1	Sterilization Requirements	13
2.2.2	Packaging Restraints	16
2.2.3	Deployment and Orientation Considerations	18
2.3	Structural Design Considerations	23
2.3.1	General Requirements and Assumptions	23
2.3.2	Applicable Environments	24
2.3.3	Design Loads for Preliminary Structural Analysis	30
3.	TASK II CONSIDERATIONS	36
3.1	Preliminary Thermal Analysis	36
3.1.1	Solar Array Thermal Environment	36
3.1.2	Solar Panel Temperature	38
3.2	Preliminary Power Analysis	42
3.2.1	Radiation Environment and Effects	42
3.2.2	Preliminary	<b>44</b>
3.3	Discussion of Possible Array Concepts	48
3.4	Aspects of Martian Environmental Effects on Material Selection	51
3.4.1	Effect of CO <sub>2</sub> Atmosphere	51
3.4.2	Effect of Dust Particles on Electrical Performance of Array	53
3.4.3	Effect of Dust Storm on Surface	55
4.	CONCLUSIONS	59

## ILLUSTRATIONS

1	Mars Thermal Environment	6
2	Mars Solar Intensity	99
3	Spectral Distribution Curves Related to the Sun at Earth. Shaded Areas Indicate Absorption, at Sea Level, Due to the Atmospheric Constituents Shown	11
4	Solar Panel Clearance Layout	17
5	Rotation Axis of Mars with Respect to Ecliptic Plane	20
6	Relationship of Local Normal Vector at $-20^{\circ}$ Latitude with Respect to the Sun Vector	21
7	Solar Array Orientation Requirements for Location at $-20^{\circ}$ Latitude of Mars	22
8	Random Vibration Test Spectrum, JPL Contract 952035	25
9	Parachute Opening Shock, JPL Contract 952035	28
10	Landing Shock	29
11	Design Loads for Launch Configuration	32
12	Martian Atmosphere Absorption of Infrared Radiation	39
13	Diurnal Temperature Variation, Equator at Perihelion	40
14	Array Concepts (stowed position)	50
15	Threshold Velocities: a) Variation of Threshold Velocity for a Range of Equivalent Surface Pressures for Silica Flour; b) Threshold Velocity for Various Sized Particles in Simulated Martian Environment	56

## SECTION 1

### INTRODUCTION

This report is the first quarterly report of the Planetary Photovoltaic Solar Array, and is in response to the requirements of JPL Contract 952035 , Paragraph 5 (iv) .

This contract covers the study of the feasibility of design for the development and fabrication of a photovoltaic solar array capable of operating on the Martian surface.

The total overall program is separated into three phases **as follows:**

- Phase I    - Feasibility Study
- Phase II   - Design and Development
- Phase III - Fabrication

This study contract covers Phase I, and is the study and analysis to provide a conceptual design of a photovoltaic solar array capable of producing 200 watts of raw electrical power on the Martian surface at solar noon.

An analysis of the program organization, responsibilities, milestones, and task breakdowns was given to JPL in the EOS initial report dated 14 August 1967.

This report finalizes the requirements of Task I, the environmental definitions of the Martian surface, and in addition gives a preliminary review of the possible concepts as defined in Task II of the program outline.

## SECTION 2

### TASK I SUMMARY

#### 2.1 MARTIAN ENVIRONMENTAL MODEL

A wealth of information on Mars environments has been generated and compiled by JPL. This information, which is quite general in nature, was given to EOS in the performance of this contract. The Martian environmental model to be presented in the following subsections is the joint JPL-EOS interpretation of the general information available. Wherever possible, our rationale for selecting a given value or parameter from a wide range of data will be given, together with the appropriate supplemental references.

##### 2.1.1 MARS ATMOSPHERE

Ten models of Martian atmosphere, as shown in Table I, have been considered as plausible in covering a wide range of experimental data. Our selection of the VM-2 model as the most probable case was based primarily on later works on spectroscopic and occultation experiments which indicated the atmosphere to consist of virtually all carbon dioxide with the surface pressure of 8 mb.\*

The parameters of the Martian atmosphere which are pertinent to the solar array study are summarized in Table II. The most probable model corresponds to the VM-2 model and the maximum-and minimum-value models correspond to the VM-8 and VM-5 models respectively. Note that the term maximum or minimum is based on the wind load effect which is approximately proportional to the product of density and (velocity)<sup>2</sup> for the low Mach number regime.

---

\*"High-Dispersion Spectroscopic Observations of Mars. I. The CO<sub>2</sub> Content and Surface Pressure," by Hyron Spinrad et al. The Astrophysical Journal, Vol. 146, No. 2, Nov 1966

TABLE I  
MARS ATMOSPHERIC MODELS (Revised)

Property	Symbol	Dimension	VM-1	VM-2	VM-3	VM-4	VM-5	VM-6	VM-7	VM-8	VM-9	VM-10
Surface Pressure	$P_0$	mb	7.0	7.0	10.0	10.0	14.0	14.0	5.0	5.0	20.0	20.0
Surface Density	$\rho_0$	lb/ft <sup>2</sup> (gm/cm <sup>3</sup> )10 <sup>5</sup> (slugs ft <sup>3</sup> )10 <sup>5</sup>	14.6 0.955 1.85	14.6 1.85 3.59	20.9 1.365 2.65	20.0 2.57 4.98	29.2 1.91 3.7	29.2 3.08 5.97	10.4 0.68 1.32	10.4 1.32 2.56	41.7 2.73 5.30	41.7 3.83 7.44
Surface Temperature	$T_0$	*K	275	200	275	200	275	200	275	200	275	200
Stratospheric Temperature	$T_s$	*R	495	360	495	360	495	360	495	360	495	360
Acceleration of Gravity at Surface	$g$	*K cm/sec <sup>2</sup> ft/sec <sup>2</sup>	200 360 375	100 180 375	200 360 375	100 180 375	200 360 375	100 180 375	200 360 375	100 180 375	200 360 375	100 180 375
Composition (percent)												
CO <sub>2</sub> (by mass)			28.2	100.0	28.2	70.0	28.2	35.7	28.2	100.0	28.2	13.0
CO <sub>2</sub> (by volume)			20.0	100.0	20.0	68.0	20.0	29.4	20.0	100.0	20.0	9.5
N <sub>2</sub> (by mass)			71.8	0.0	71.8	0.0	71.8	28.6	71.8	0.0	71.8	62.0
N <sub>2</sub> (by volume)			80.0	0.0	80.0	0.0	80.0	32.2	80.0	0.0	80.0	70.5
A (by mass)			0.0	0.0	0.0	30.0	0.0	35.7	0.0	0.0	0.0	25.0
A (by volume)			0.0	0.0	0.0	32.0	0.0	38.4	0.0	0.0	0.0	20.0
Molecular Weight	$M$	mol <sup>-1</sup>	31.2	44.0	31.2	42.7	31.2	36.6	31.2	44.0	31.2	31.9
Specific Heat of Mixture	$C_p$	cal/gm °C	0.230	0.166	0.230	0.1530	0.23	0.174	0.230	0.166	0.230	0.207
Specific Heat Ratio	$\sigma$		1.38	1.37	1.38	1.43	1.38	1.45	1.38	1.37	1.38	1.41
Adiabatic Lapse Rate	$\Gamma$	*K/km *R/1000 ft	-3.88 -2.13	-5.39 -2.96	-3.88 -2.13	-5.85 -3.21	-3.88 -2.13	-5.14 -2.82	-3.88 -2.13	-5.39 -2.96	-3.88 -2.13	-4.33 -2.38
Tropopause Altitude		km kilo ft	19.3 63.3	18.6 61.0	19.3 63.3	17.1 56.1	19.3 63.3	19.4 63.6	19.3 63.3	18.6 61.0	19.3 63.3	23.1 75.8
Inverse Scale Height (stratosphere)		km <sup>-1</sup>	0.0705	0.199	0.070	0.193	0.0705	0.1655	0.0705	0.199	0.0705	0.145
Free Stream Continuous Surface Wind Speed	$\bar{v}$	ft <sup>-1</sup> x 10 <sup>5</sup>	2.15	6.07	2.15	5.89	2.15	5.05	2.15	6.07	2.15	4.41
Maximum Surface Wind Speed*	$v_m$	ft/sec	186.0	186.0	156.0	156.0	132.0	132.0	220.0	220.0	110.0	110.0
Design Gust Speed	$v_g$	ft/sec	380.0	380.0	310.0	310.0	270.0	270.0	450.0	450.0	225.0	225.0
			200	200	150.0	150.0	150.0	150.0	200.0	200.0	100.0	100.0

\*N.B. The values given here are lower than those given in Revision 1.

**TABLE II**  
**MARS ATMOSPHERIC CONSIDERATIONS**

<u>Property</u>	<u>Dimension</u>	<u>Probable Model</u>	<u>Maximum-Value Model</u>	<u>Minimum-Value Model</u>
Surface pressure	mb	7.0	5.0	14.0
Surface density	(gm/cm <sup>3</sup> )10 <sup>5</sup>	1.85	1.32	1.91
Surface temperature	°K	200	200	275
Stratospheric temperature	°K	100	100	200
CO <sub>2</sub> (by mass)	%	100	100	28.2
N <sub>2</sub> (by mass)	%	0.0	0.0	71.8
A (by mass)	%	0.0	0.0	0.0
Molecular weight	MOL <sup>-1</sup>	44.0	44.0	31.2
Specific heat ratio	cal/gm° C	0.166	0.166	0.23
Specific ht ratio	-	1.37	1.37	1.38
Adiabatic lapse rate	°K/km	-5.39	-5.39	-3.88
Tropopause altitude	km	18.6	18.6	19.3
Free stream cont. surface wind speed	ft/sec	186	220	132
Maximum surface wind speed	ft/sec	380	450	270
Design gust speed	ft/sec	200	200	150



### 2.1.2 THERMAL ENVIRONMENT

Since the Martian atmosphere was assumed to be 100 percent CO<sub>2</sub> at a pressure of 7 mb, the mode of heat transfer from the spacecraft to environment will be both radiation and convection. The heat transfer parameters of interest are the soil surface emissivity, the atmospheric albedo, and the daily surface temperature variation.

These parameters were summarized in Fig. 1. The probable values of emissivity and albedo are 0.85 and 0.15 respectively. The temperature variations are shown to be a function of latitude and they correspond to the Martian winter condition. The surface temperature in the summer is expected to be 12°K higher than the winter condition. Daily temperature fluctuation is approximately 100°C.

### 2.1.3 CLOUDS AND DUST

The information on cloud and dust conditions on Mars is sketchy and speculative in nature. Such information has been summarized in Table 111. The concern on the solar array performance as affected by the Martian clouds and dusts falls into two areas. The first area is the realistic estimate of the solar intensity at the surface as a result of atmospheric attenuation. This subject will be discussed in the next section. The second area is concerned with the effect of settling dusts on the optical properties of the solar cell cover glass, the possibility of conductive dust particles shorting the exposed electrical contacts, and finally the effect of dust storms on the cover glass and thermal coating deterioration. This latter area will be covered in Subsection 3.4.

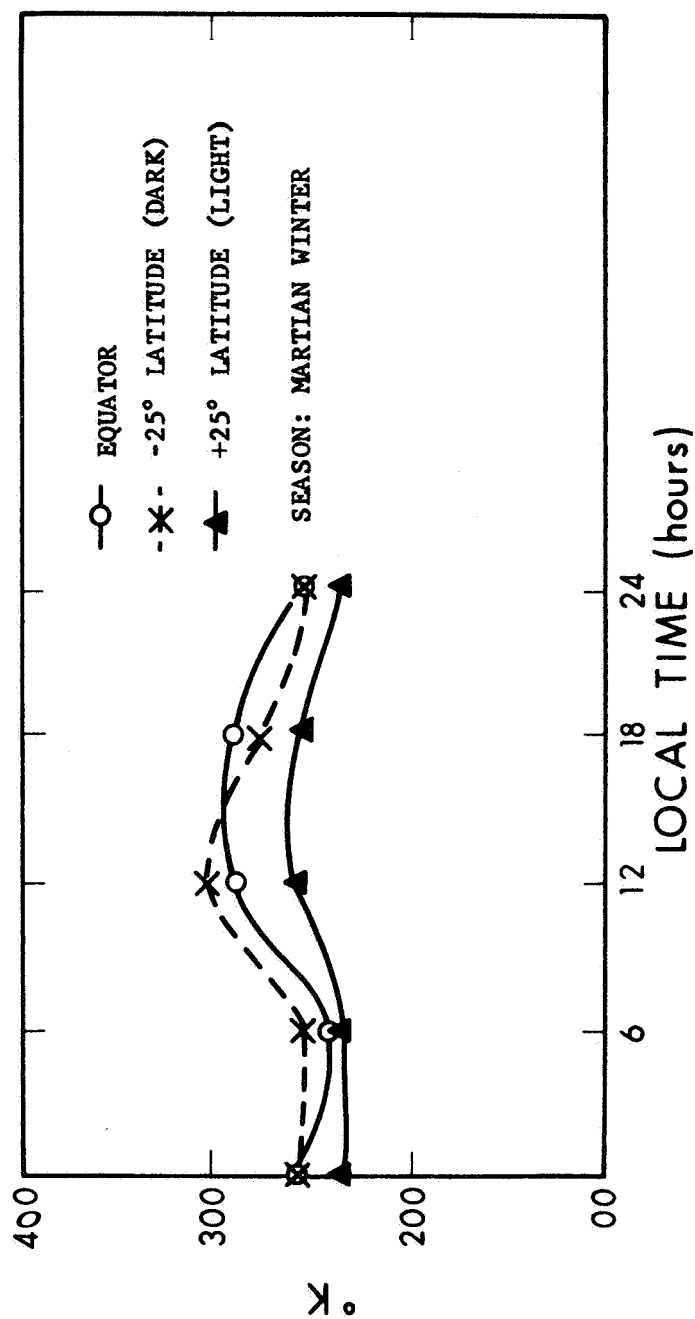


Figure 1. Mars Thermal Environment

TABLE III  
MARTIAN CLOUDS AND DUST CONSIDERATIONS

- Yellow clouds
  - Altitude - 3-30 km
  - Particle size - 1-100 $\mu$
- Blue clouds
  - Altitude - Unknown at present
  - Particle size - 0.1 $\mu$
  - Material - H<sub>2</sub>O ice crystals and condensed violet material (4550Å)
- White clouds
  - Altitude - 15-25 km
  - Particle size - 1 $\mu$
  - Material - H<sub>2</sub>O or CO<sub>2</sub> ice crystals
- Entrained dust
  - Altitude - Dependent upon wind speeds
  - Particle size - 1-1000 $\mu$
  - Material density - 2-4 gm/cc
  - Airborne threshold velocity - 200-300 ft/sec

#### 2.1.4 SOLAR INTENSITY

The solar intensity near Mars space varies from 50 to  $74 \text{ mW/cm}^2$ , depending on the distance from Mars to the sun. For the intensity at the surface, a rough engineering estimate was made to determine the transmission factor, which was found to be approximately 92 percent.

Attempts to perform a more accurate calculation proved to be unfruitful as the uncertainties of several parameters which enter into the attenuation process are large. The following discussion describes the degree of uncertainty of several contributing parameters:

- a. The attenuation of the solar photon by the atmosphere consists of two basic processes, i.e., scattering and absorption. Three components which are responsible for scattering are  $\text{CO}_2$  gas molecules, dust particles, and water vapor. Of the three components, only gas molecule scattering can be computed with any accuracy.
- b. Of the two components responsible for absorption, water vapor and  $\text{CO}_2$ , only the latter's contribution can be calculated. Since  $\text{CO}_2$  absorption occurs mostly at wavelengths longer than  $2.5\mu$ , it can be neglected for reason that the integrated solar energy at  $\lambda > 2.5\mu$  will contribute only approximately 2 percent of the total energy.

The approach taken was to assume that the attenuation is a logarithmic function of the pressure. By analogy with Earth conditions, we assigned a transmission factor of 0.7 at a pressure of 1000 mb (Earth AMI value). The transmission factor at 1 mb was assumed to be 1.0. By logarithmic extrapolation, the transmission factor at Mars surface (7 mb) was found to be 0.92. This is shown in Fig. 2.

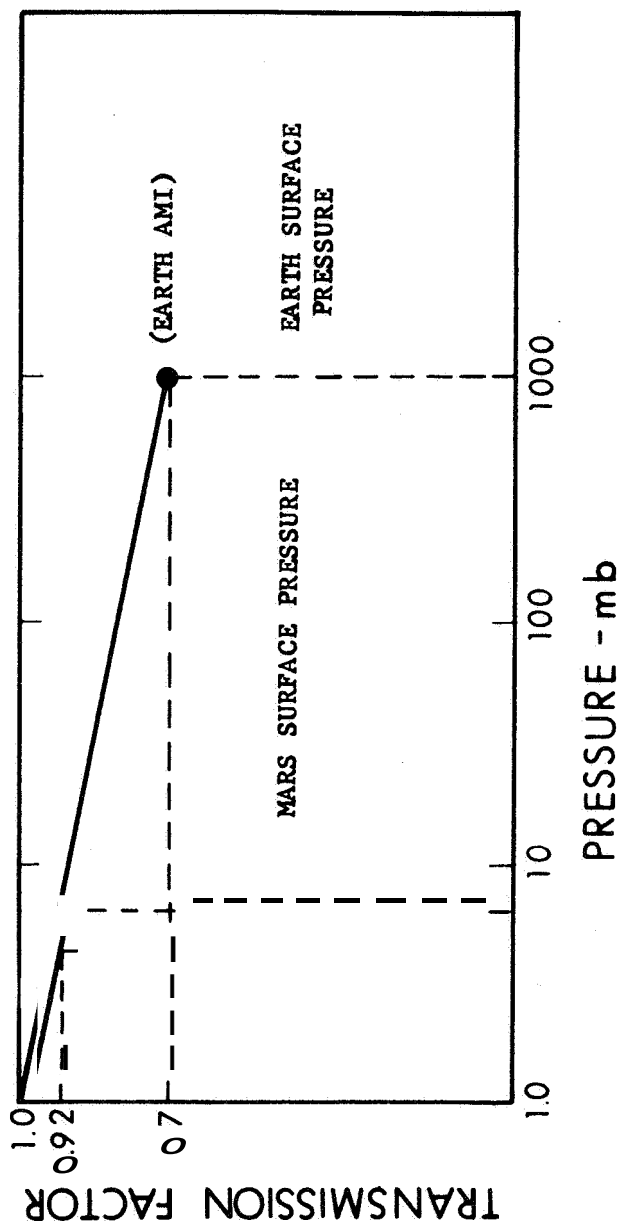
We believe the assumption leading to the recommended transmission factor to be a conservative one. This is due to the fact that the Martian atmospheric contents of  $\text{O}_2$ ,  $\text{O}_3$ , and water vapor, are significantly

● NEAR MARS SPACE: 50 TO 74  $\text{mW/cm}^2$

● AT MARS SURFACE:

RECOMMENDED TRANSMISSION FACTOR AT AIR MASS ONE = 0.92

● RATIONALE:



● JUSTIFICATION:

- ONLY GAS MOLECULE SCATTERING CAN BE COMPUTED
- WATER VAPOR SCATTERING - UNKNOWN
- DUST SCATTERING - UNKNOWN
- WATER VAPOR ABSORPTION - UNKNOWN
- CO<sub>2</sub> ABSORPTION CAN BE CALCULATED, BUT IT MAY BE NEGLECTED AS IT OCCURS AT LONG WAVELENGTHS ( $> 2.5 \mu$ )

Figure 2. Mars Solar Intensity

lower than those on Earth. Since these components are principally responsible for absorption as illustrated in Fig. 3, our assumption of logarithmic absorption analogous to Earth conditions will certainly be conservative.

#### 2.1.5 RADIATION ENVIRONMENT

Assuming that no artificial radioactive source such as an RTG is attached to the surface laboratory, the radiation damage to the solar cells will be due only to natural sources of galactic and solar cosmic radiation. To quote from JPL documents, these sources are:

- a. Galactic cosmic radiation. The galactic cosmic radiation near Mars consists of essentially the proton component and its secondary radiation produced in the Martian atmosphere. The radiation dose rate at the top of the Martian atmosphere ranges between 20 and 45 mr/day. The dose rate at the surface of Mars ranges between 10 and 25 mr/day; this range is based on an average 10 mb surface atmosphere producing approximately 30 gm/cm<sup>2</sup> of mass attenuation. A change in the value of the surface pressure by 5 mb affects the dose rate by only about 10 percent. The radiation due to natural radioactivity will be a small fraction of that due to cosmic radiation.
- b. Solar cosmic radiation. The range of the surface atmospheric pressure of Mars corresponds to a range of atmospheric mass per unit area of 11 to 44 gm/cm<sup>2</sup>. The solar cosmic proton radiation is much more sensitive than galactic cosmic radiation to this range of mass attenuation because of the lower energy protons in the solar cosmic radiation. The approximate attenuations of the free space spectra, yielding surface time-integrated fluxes of the model solar flare event and the maximum yearly flux of solar flare events at 1.5 AU from Sun are given in Table IV.

#### 2.1.6 SUMMARY OF MARS PROBABLE ENVIRONMENTAL MODEL

The pertinent parameters of the Martian environment in connection with the solar array study are summarized in Table V.

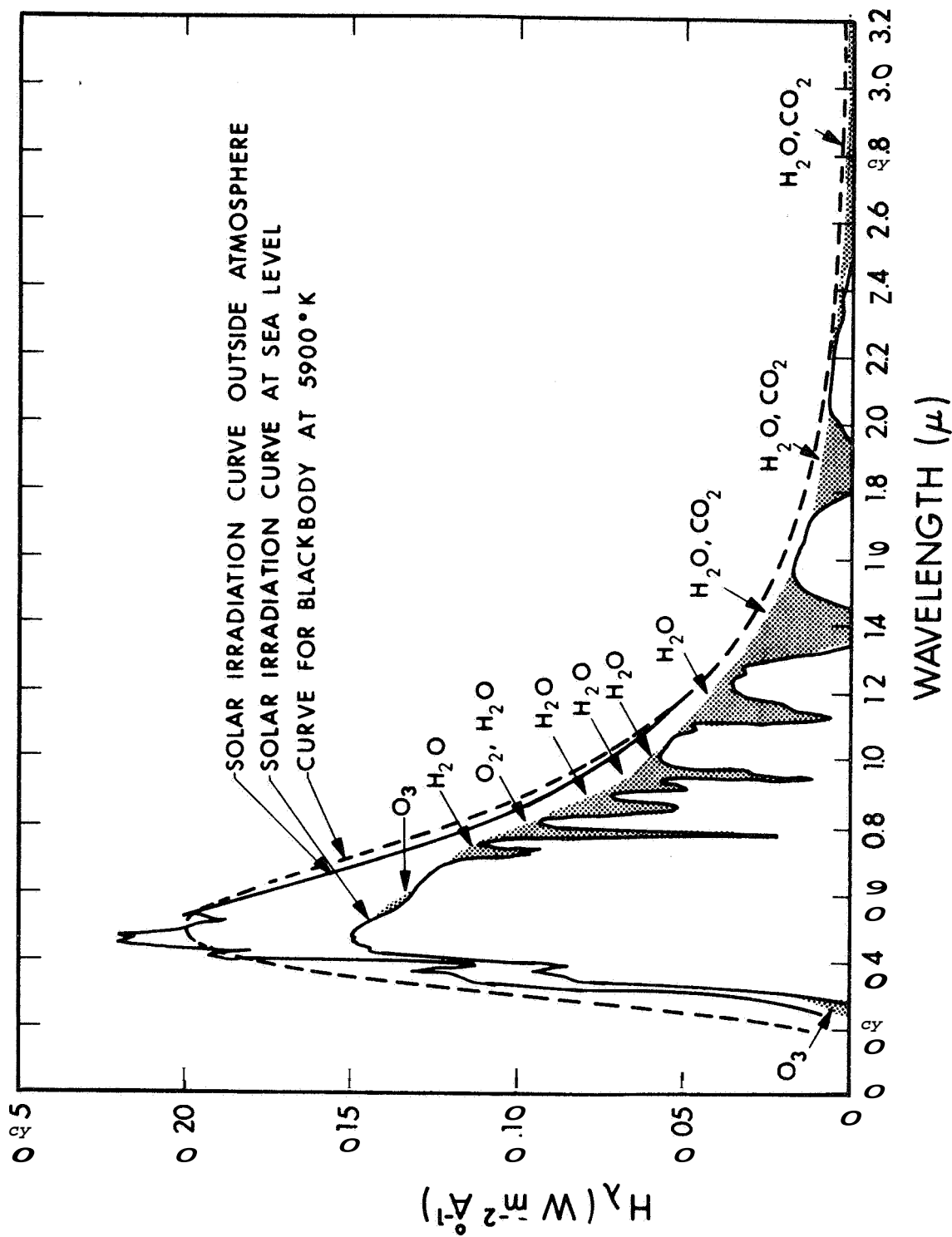


Figure 3. Spectral Distribution Curves Related to the Sun at Earth. Shaded Areas Indicate Absorption, at Sea Level, Due to the Atmospheric Constituents Shown.

TABLE IV

MAXIMUM TIME-INTEGRATED PROTON FLUX			
	Energy (Mev)	Flux (protons/cm <sup>2</sup> ) Atmospheric Mass Attenuation	
		(11 gm/cm <sup>2</sup> )	(44 gm/cm <sup>2</sup> )
Maximum Time-Integrated Proton Flux per Flare	E > 10	1.2 x 10 <sup>8</sup>	3.2 x 10 <sup>7</sup>
	E > 30	9.8 x 10 <sup>7</sup>	2.9 x 10 <sup>7</sup>
	E > 100	6.7 x 10 <sup>7</sup>	2.7 x 10 <sup>7</sup>
Maximum Time-Integrated Proton Flux per Year	E > 10	1.6 x 10 <sup>8</sup>	5.3 x 10 <sup>7</sup>
	E > 30	1.3 x 10 <sup>8</sup>	4.9 x 10 <sup>7</sup>
	E > 100	9.3 x 10 <sup>7</sup>	4.4 x 10 <sup>7</sup>

TABLE V

## MARS PROBABLE ENVIRONMENTAL MODEL

## • Atmosphere

Pressure: 7 mb  
 Atmos gas: ~ 100% CO<sub>2</sub>  
 Wind speed (0.8  $\bar{V}$ ): 150 ft/sec (10 M height)  
 Maximum wind speed: 380 ft/sec

## • Thermal environments

Albedo: 0.15  
 Emissivity: 0.85  
 Maximum temperature: 312°K  
 Minimum temperature: 150°K  
 Daily variation: 100°K

## • Dust storms

Periodic occurrence, probably when wind gusts exceed 300 ft/sec

## • Solar intensity

Near Mars space: 50-74 mW/cm<sup>2</sup>  
 Transmission factor at surface, AMI = 0.92

## • Radiation

Galactic cosmic radiation: 10-25 mr/day  
 Solar cosmic radiation: Ref. Table IV



## 2.2 MISSION RESTRAINTS

### 2.2.1 STERILIZATION REQUIREMENTS

JPL has specified that the feasibility study of the solar array design shall include consideration of array sterilization.

The solar arrays destined to enter the Martian atmosphere and land on the Martian surface shall be biologically sealed in a sterilization canister and remain sealed through the terminal heat sterilization cycle. After sterilization, the canister shall remain biologically sealed until it is separated in flight in the vicinity of Mars. Prior to the terminal heat sterilization cycle, the equipment will be processed in a manner to minimize the biological contamination, and will receive an ethylene oxide (ETO) decontamination.

#### 2.2.1.1 Part and Material Qualification

In order to promote uniformity of testing, the test levels given in Tables VI and VII are recommended for parts and material qualification. It is not a requirement that all parts and materials intended to be used in the flight capsule be qualified to these test levels. Ultimately, the acceptability of the various parts and materials comprising the capsule will be based on the results of subsystem and system type approval testing.

#### 2.2.1.2 Sterilization Test Levels

The test levels applicable to solar array qualification and acceptance and capsule terminal sterilization shall be as given in Tables VI and VII.

	Temp (°C)	ETO Concentration mg/liter	Relative Humidity (%)	Exposure Time (hr/cycle)	No. of Cycles
Parts and materials qualification*	50	600	50	**	**
Subsystem (assembly) testing					
FA	40	500	40	**	**
TA	50	600	50	**	**

\*Optional test

\*\*To be determined later

TABLE VII  
HEAT STERILIZATION PARAMETERS

	Temp (°C)	Chamber Nitrogen Concentration	Exposure Time (hr/cycle)	No. of Cycles
Parts and materials qualification*	135	**	**	**
Subsystem (assembly) testing				
FA	125	**	**	**
TA	135	**	**	**

#### 2.2.1.3 Ethylene Oxide (ETO) Decontamination

Those capsule elements undergo TA, FA, or compatibility testing shall be subjected to ETO decontamination in an enclosed test chamber capable of producing a controlled environment of time, temperature, temperature rate, relative humidity (RH), pressure decay, and specified ETO concentration as defined for the appropriate test item and environment. The ETO decontaminating agent shall contain 12 percent ETO and 88 percent **dichloro-defluoro-methane** (Freon 12 or Genetron 12) by weight.

#### 2.2.1.4 Heat Sterilization Tests

Those capsule elements undergoing TA, FA, or compatibility testing shall be subjected to heat sterilization testing in an enclosed test chamber capable of producing a controlled environment of time, temperature, and temperature rate as defined for the appropriate test item and environment. The gas used for all heat sterilization test shall be nitrogen.

#### 2.2.1.5 Type Approval (TA) Testing

TA tests are those tests which demonstrate the adequacy of the design for its intended usage, including performance, margin, and other similar tests. The TA tests are formal, and although much development testing may precede them, they are considered to be the actual demonstration of satisfactory design. TA tests are performed both on the capsule proof test model (**PTM**) and on prototypes of all subsystems or assemblies. The TA tests shall be performed on equipment in the same configuration as is intended for FA tests and any subsequent design change or FA configuration change shall, in general, invalidate the TA tests. Units subjected to TA tests are automatically disqualified for flight. The TA tests are not intended to be destructive tests; to successfully pass them, equipment shall function in accord with its detail specification.

#### 2.2.1.6 Flight Acceptance (FA) Testing

FA tests are those tests which demonstrate that the hardware is ready for flight. These tests are complements of the TA tests, although they are not as extensive. They include performance tests, environmental tests, margin tests, and other related tests. The FA tests complement activities such as inspection and calibrations. The FA tests are formal and, although much calibration and related work is done, they are the tests by which the unit is certified ready for flight. FA tests are to be conducted on identical TA equipment configurations and subsequent rework of the equipment shall, in general, invalidate the FA tests. Limits as shall be placed on the number of times any one serial-numbered equipment undergoes FA environmental testing.

#### 2.2.2 PACKAGING RESTRAINTS

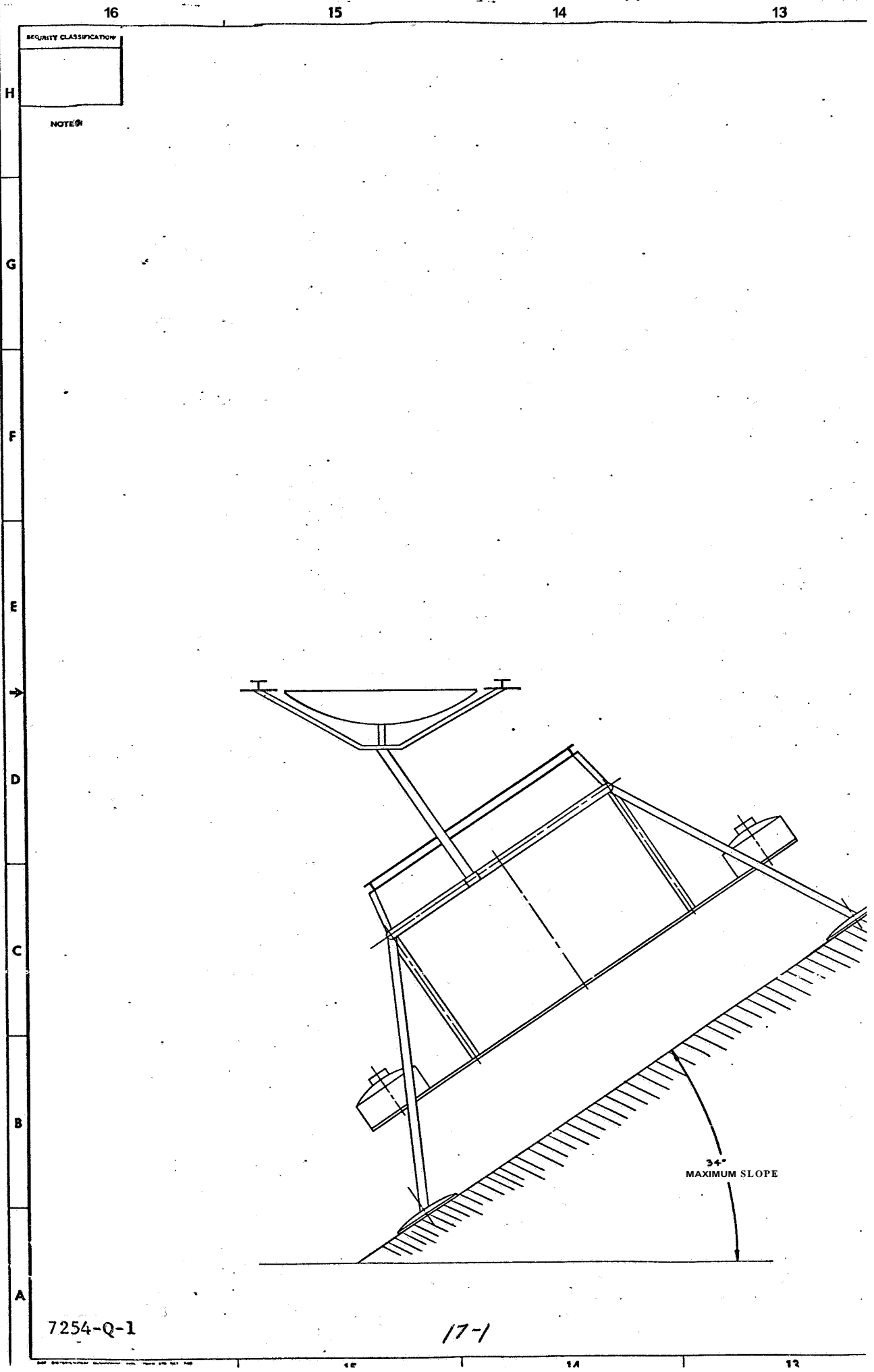
The packaging restraints are defined as those restraints imposed on the solar array by the physical configuration of vehicle and sterilization canister while in the launch, transit, and landing mode.

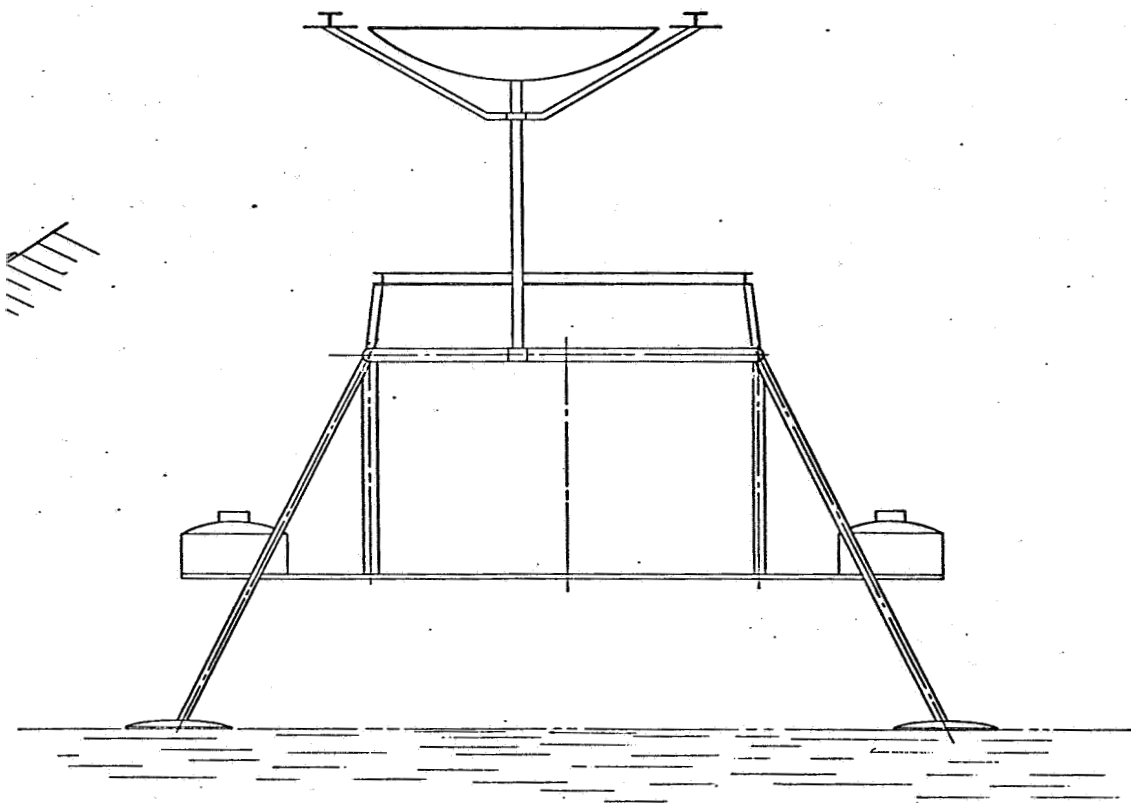
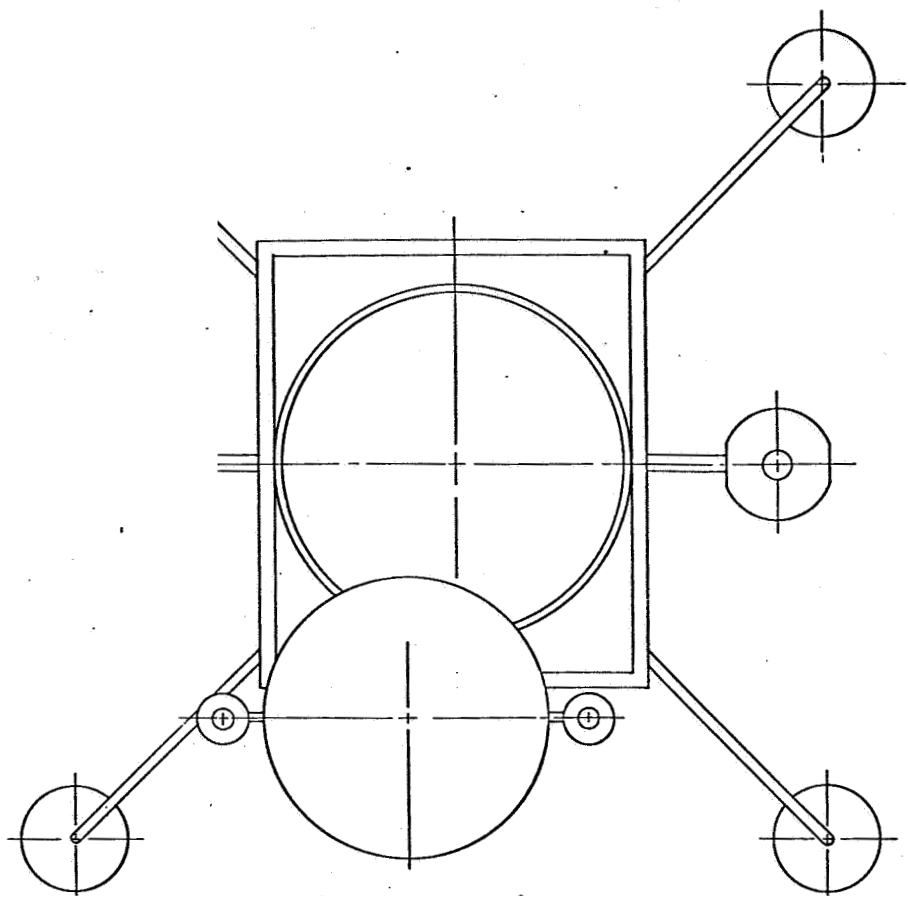
This configuration is depicted by JPL drawing 10652002 as furnished by JPL as a part of this contract, and by EOS drawing 7254-100 (Fig. 4) which further develops the detail of the spacecraft.

Preliminary analysis of the packaging restraints shows that the following panel areas can be contained within the limitations depicted:

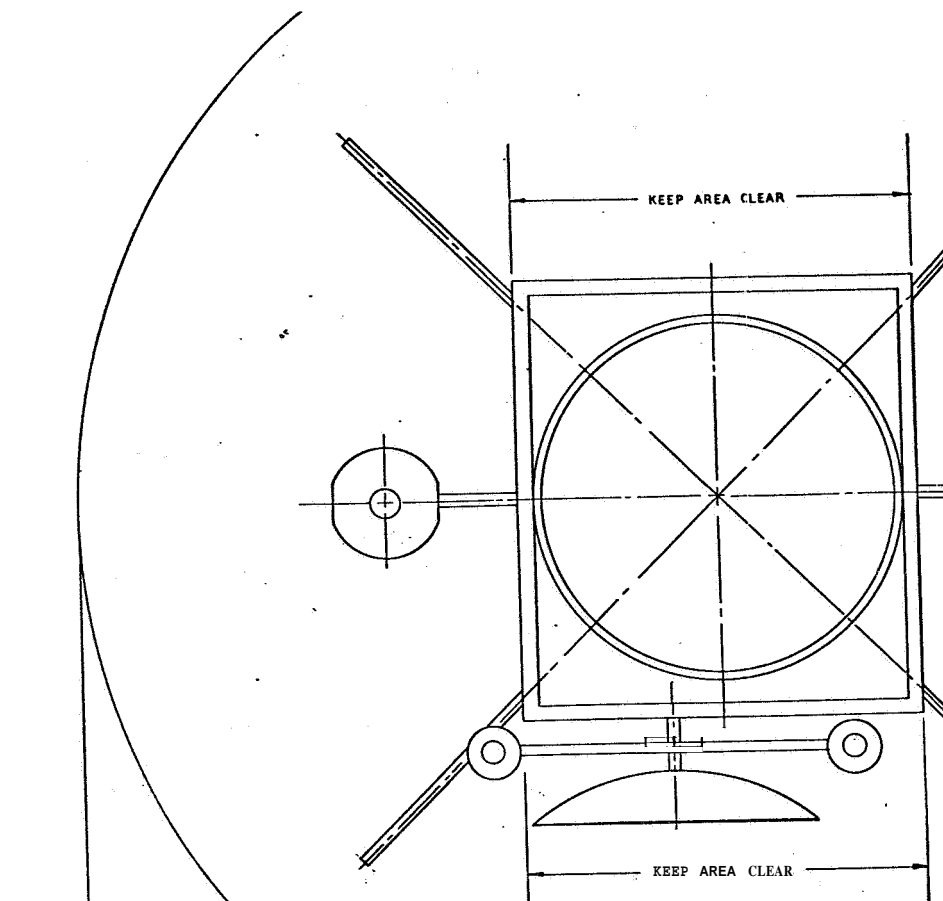
- a. Flat nonfolded arrays, approximately 85 sq ft per side of the spacecraft body, for a total of 190 sq ft of solar array. This would involve a panel with a curved outer edge on an approximate 110 inch radius.
- b. Conical circumferential fixed array, approximately 260 sq ft total panel area with a major diameter of 220 in., and a minor diameter of 120 in., with panel surface length of 70 in.

DATE: 1/24/71





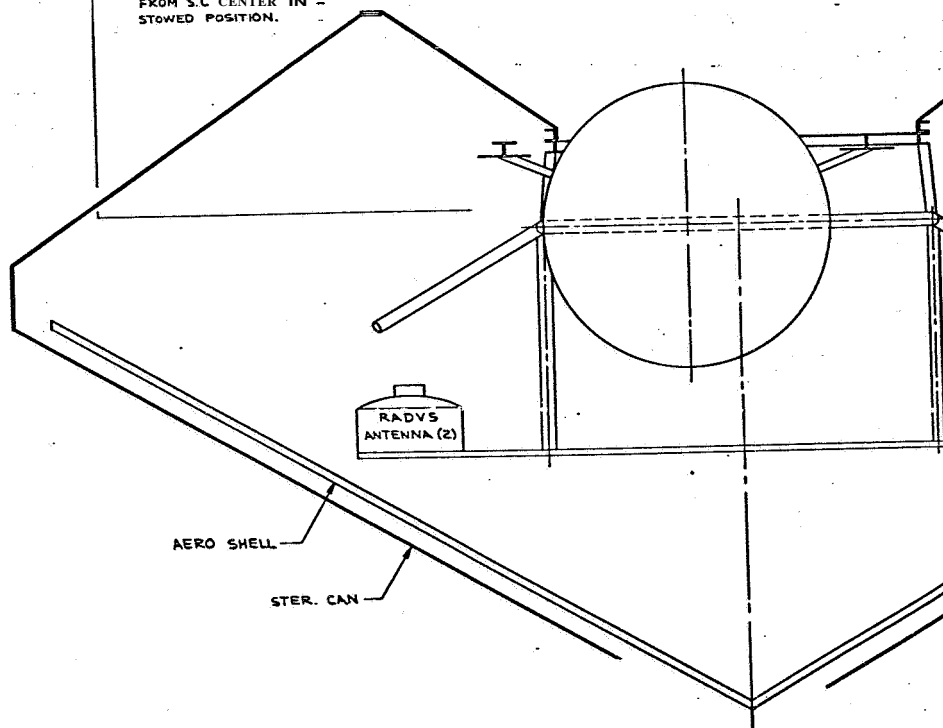
EXTENDED POSITION



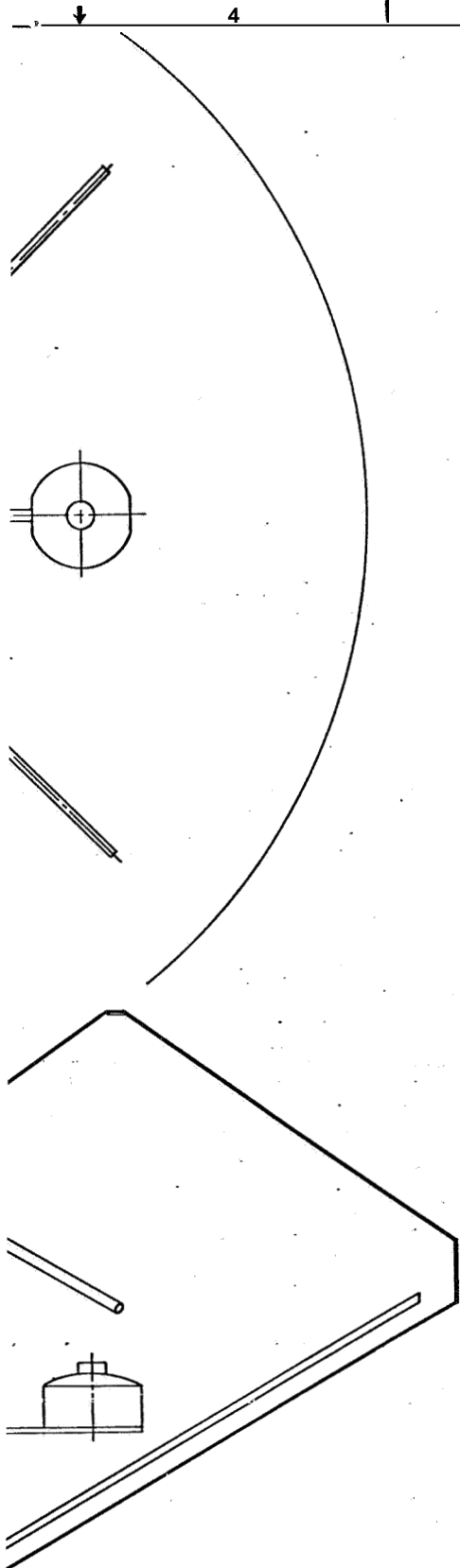
**TOP VIEW**  
**STOWED CONDITION**

AREA AVAILABLE

FOR S.P. IN STRAIGHT  
OUT POSITION. 107" R  
FROM S.C. CENTER IN  
STOWED POSITION.



**SIDE VIEW**  
**STOWED CONDITION**



REVISIONS			
NO.	DESCRIPTION	DATE	APPROVED
1			

H  
G  
F  
E  
D  
C  
A

17-4

SCALE-INCHES  
0 10 20 30 40 50 60

SYM	CODE	PART OR IDENTIFYING NO.	NOMENCLATURE OR DESCRIPTION	MATERIAL	SPECIFICATION	UNIT WT.	ZONE	ITEM NO.
QTY REQD								
UNLESS OTHERWISE NOTED								
LINEAR DIMS. IN INCHES								
TOLERANCES								
DECIMAL FINISH ANGULAR								
.005 ± .005 ±								
.002 ± .002 ±								
DO NOT SCALE								
MATERIAL								
WFG								
DESIGN ACTIVITY APPD								
SIMILAR TO ACT. WT. SCALE WT. CUSTOMER								
TREATMENT/FINISH								
CONTRACT NO. DATE								
DRAWN BY: [Signature] CHECKED BY: [Signature]								
ELECTRO-OPTICAL SYSTEMS, INC.								
A Subsidiary of Santa Barbara								
300 N. Main Street, Pasadena, California, 91107								
TITLE								
LAYOUT -								
SOLAR PANEL CLEARANCE								
Dwg No. 12705								
Dwg No. 7254-100								
SCALE NOTED RELEASE DATE								
SHEET								

Figure 4.



- c. A volume of 64 cu ft per side of the vehicle body can readily be obtained for possible storage of a undeployed folding or roll-up array.

The preliminary study of the package restraints indicate that sufficient area or volume is available within the design limitations as expressed by JPL to satisfy the physical size of any of the six array concepts presently under consideration.

### 2.2.3 DEPLOYMENT AND ORIENTATION CONSIDERATIONS

In this section, factors which must be taken into deployment and orientation considerations will be discussed. The pertinent ground rules having a strong influence in the selection of the array concept are the following:

1. The surface laboratory is intended to land on the equator, but the design must accommodate a landing error of  $\pm 20^\circ$  in latitude.
2. The maximum terrain slope is  $34^\circ$ .
3. The surface laboratory cannot provide any slope leveling capability.
4. Once landed, the surface laboratory cannot be reoriented to have a preferred orientation toward the sunrise-sunset line (east-west of Mars).
5. Two opposing sides of the laboratory not used for the array attachment are to be kept clear. This requirement is probably put forth to reserve a clear view from the laboratory to Mars surface for some scientific instrumentation.

#### 2.2.3.1 Ground Rules No. 4 and 5

Ground rule No. 4 does not permit the vehicle to move to position the array to the no-shadow E-W line (assuming the array is not allowed to rotate around the vehicle).

Considerations have been given to rotating the array with respect to the vehicle so that the array will be aligned with the E-W line. However, the array will interfere with the other scientific instruments which may be located in the areas to be kept clear as specified by ground rule No. 5.

For the array which is mounted from the side of the surface laboratory, it appears that a 3-axis articulation is not preferred. However, this restriction does not apply for a surveyor-type panel where the panel is mounted on a vertical boom.

#### 2.2.3.2 Ground Rules No. 1, 2, and 3

Figures 5, 6, and 7 show the logical sequence of what will be required to satisfy the three ground rules if the spacecraft landed at  $-20^{\circ}$  latitude. This is the worst case where the total array orientation required is  $76^{\circ}$ . The breakdown of the total is:

Inclination from ecliptic plane	$22^{\circ}$
Error in landing in southern hemisphere	$20^{\circ}$
Terrain slope (N-S)	<u><math>34^{\circ}</math></u>
Total	$76^{\circ}$

In case the terrain slope is in the E-W direction, a two-axis correction will be required, i.e.,  $42^{\circ}$  correction for latitude and plane of ecliptic, and  $34^{\circ}$  for slope.

#### 2.2.3.3 Antenna Shadowing

The present spacecraft concept calls for the antenna location to be on top of the surface laboratory. Since the Earth and Mars are essentially on the same ecliptic plane, the movement of the antenna will also be

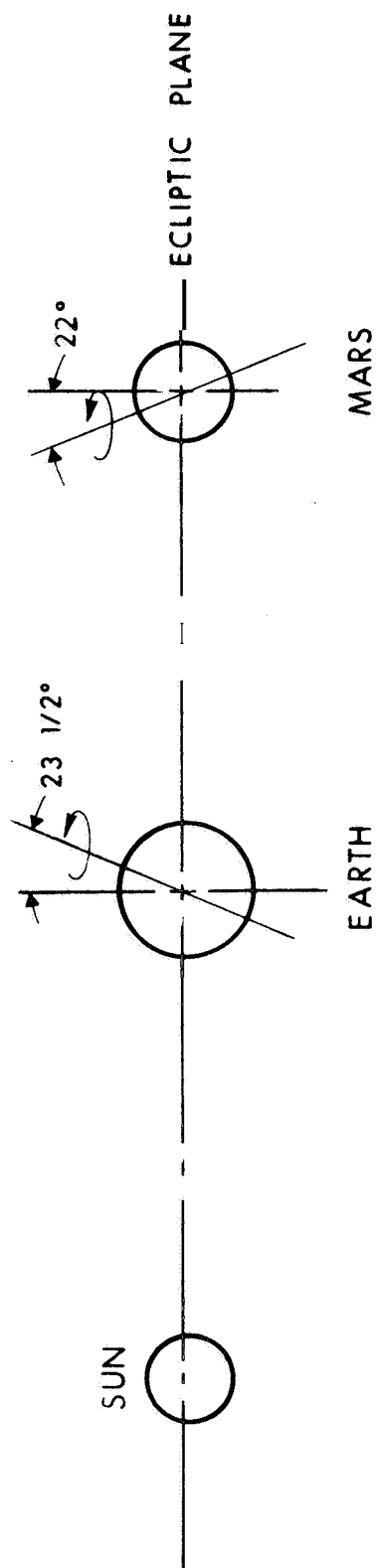


Figure 5. Rotation Axis of Mars with Respect to Ecliptic Plane

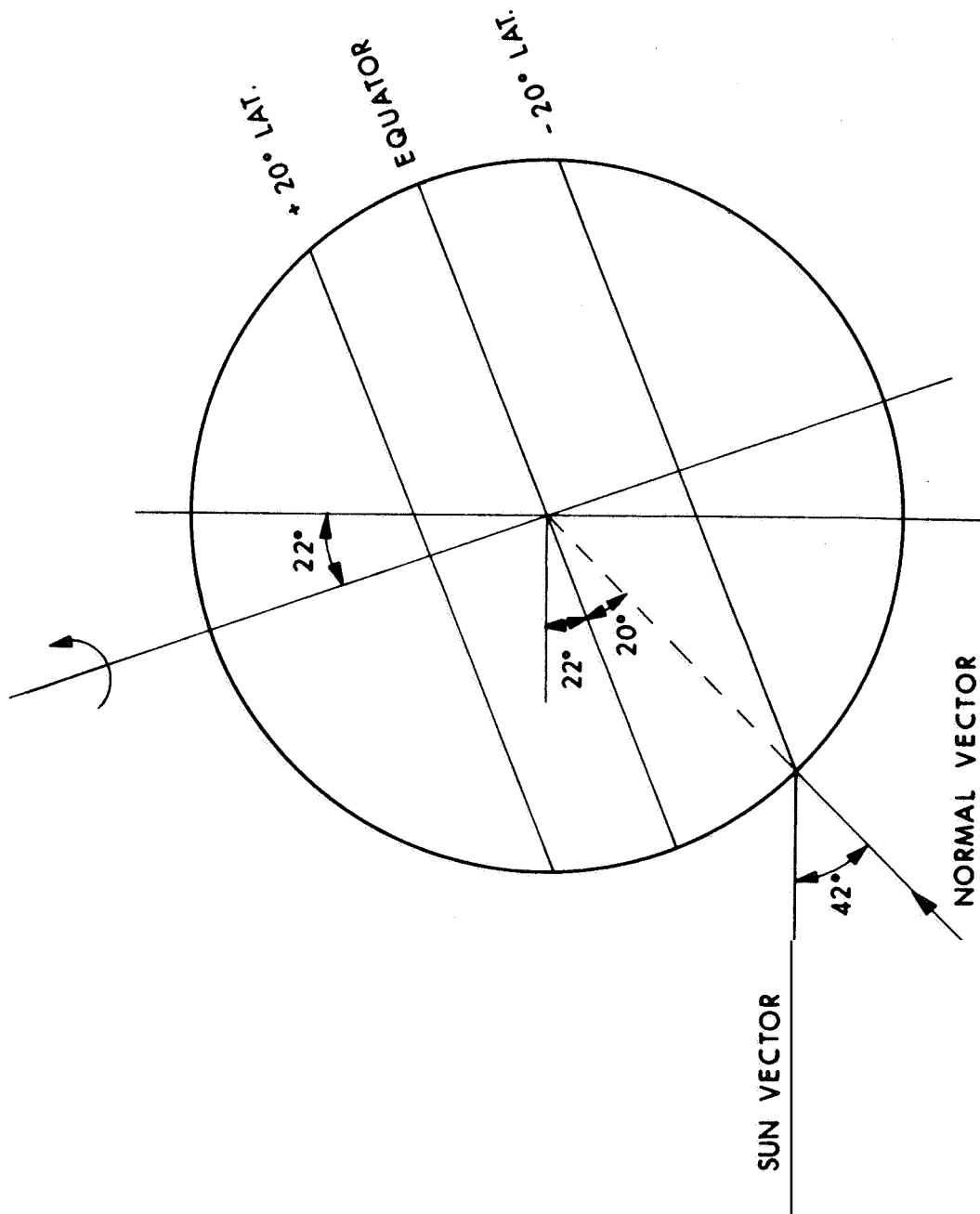


Figure 6. Relationship of Local Normal Vector at  $-20^\circ$  Latitude with Respect to the Sun Vector

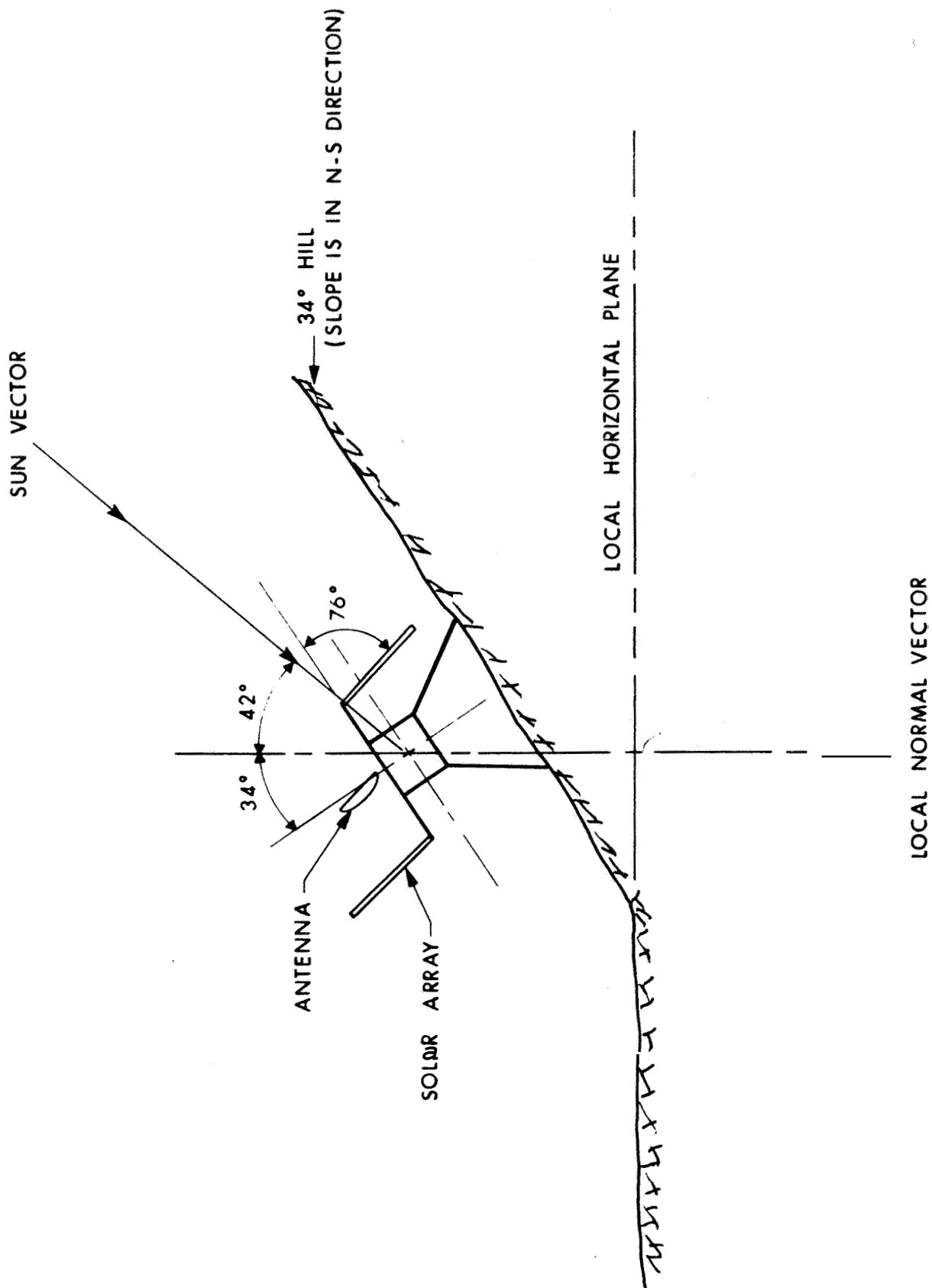


Figure 7 Solar Array Orientation Requirements for Location at  $-20^\circ$  Latitude of Mars

in this plane. However, the antenna pointing vector may be at an angle of  $\pm 40^\circ$  with the sun vector depending on the relative positions of Mars and Earth.

To avoid complete shadowing, each of the two panels will have to be mounted on a boom which is sufficiently long to clear the shadows. Again, what is shown in Fig. 7 will be the worst case.

To summarize, the deployment and orientation considerations suggest that a minimum of two-axis orientation will be required in order to meet the landing latitude error and slope requirements. It is preferable to have a 3-axis orientation capability. The advantages of the 3-axis concept are: (1) ability to align the panel in E-W direction and avoid antenna shadowing completely, (2) daily sun tracking ability so that the power profile is flat, and (3) ability to correct for latitude and slope. A 3-axis concept will, however, violate ground rules No. 4 and 5. An exception to this will be a Surveyor-type panel. Various array concepts will be discussed in more detail in Subsection 3.3.

## 2.3 STRUCTURAL DESIGN CONSIDERATIONS

### 2.3.1 GENERAL REQUIREMENTS AND ASSUMPTIONS

The ultimate design load will be **1.25** times the design load. The entire structure shall be capable of withstanding the ultimate design loads without failure.

The structure shall not yield under the design loads.

Allowable stress data shall be obtained from the Mil Handbook 5, Metallic Materials and Elements for Flight Vehicle Structures, or Mil Handbook 17, Plastics for Flight Vehicles.

All environments which are defined for the planetary vehicle will be assumed to act at the solar array-capsule mechanical interface. Dynamic loads will be considered omnidirectional.

The loads analysis will assume that the array is dynamically decoupled from the flight vehicle.

The array shall be deployable in a 1 g (Earth) environment.

### 2.3.2 APPLICABLE ENVIRONMENTS

The following environments are the basis for the generation of the structural design and material selection criteria.

#### 2.3.2.1 Low Frequency Vibration

- a. At launcher release, the longitudinal acceleration is 2.1 g (o-p) composed of transients at discrete frequencies between 4 and 45 Hz. They are described as decaying sinusoids of 20 cycles duration.
- b. At SIC shutdown, the longitudinal acceleration is a composite signal of 1.25 g (o-p) composed of transients at discrete frequencies between 6 and 70 Hz. They are described as decaying sinusoids of 20 cycles duration. Lateral environment during this event is unknown at this time.

#### 2.3.2.2 Random Vibration

The random vibration spectrum during launch is described in Fig. 8.

#### 2.3.2.3 Ignition, Staging, and Separation Shock

The shock response due to these environments is approximated by an input consisting of a 200-g terminal peak sawtooth of 0.7 to 1.0 milli-second rise time.

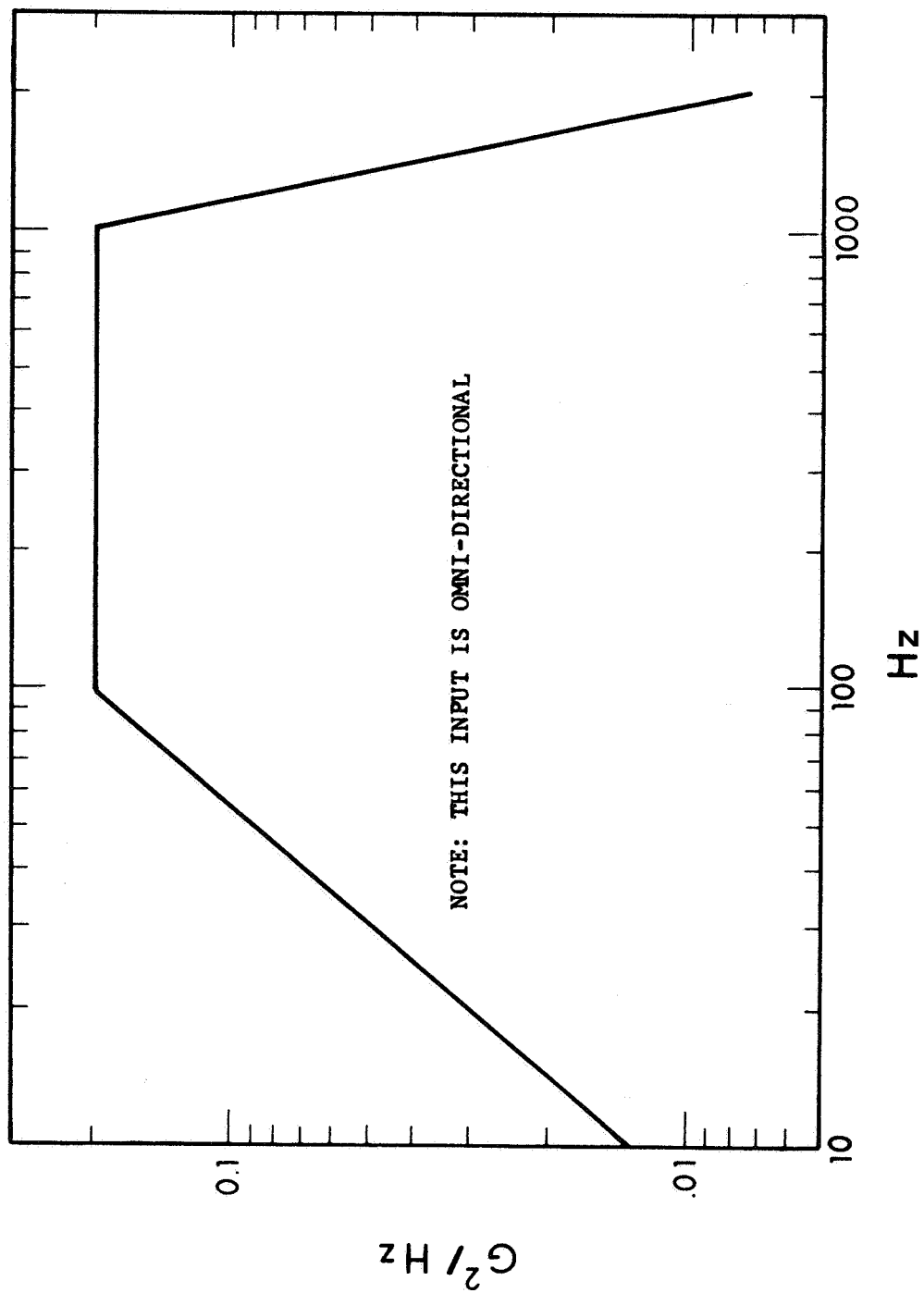


Figure 8. Random Vibration Test Spectrum, JPL Contract 952035



#### 2.3.2.4 Acoustic Noise

Overall sound pressure level of approximately 151 dB for approximately 30 seconds with a one-third octave, sound pressure level of 141, 5 dB from 80 Hz to 125 Hz with a rolloff of 5 dB/octave above 125 Hz and a rolloff of 2 dB/octave below 80 Hz.

#### 2.3.2.5 Static Accelerations

The maximum quasi-static acceleration along the thrust axis of the vehicle is 4.75 g. The lateral acceleration is less than 1 g.

#### 2.3.2.6 Aero Dynamically Induced Heating

The maximum heat flux from the shroud to the solar panel during launch is 40 watts/ft<sup>2</sup>.

#### 2.3.2.7 Ascent Pressure Environment

The ascent pressure environment is defined by the following table:

<u>Ambient Pressure versus Time</u>	
<u>Time of Flight (sec)</u>	<u>Ambient Pressure (psi)</u>
0	14.5
10	14.0
20	13.2
30	11.8
40	9.5
50	6.6
60	4.3
70	2.5
80	1.4
90	0.7
100	0.4

#### 2.3.2.8 Entry Into ~~Mars~~ Atmosphere

The aerodynamic drag upon entry into the ~~Mars~~ atmosphere will produce a quasi-static deceleration of 22.9 g.

#### 2.3.2.9 Parachute Opening Shock

The parachute opening shock is defined by Fig. 9.

#### 2.3.2.10 Landing Shock

The expected landing shock is defined by Fig. 10.

#### 2.3.2.11 Sterilization

The sterilization requirements are defined in Subsection 2.2.1.

#### 2.3.2.12 Ground Handling

The ground handling environment will be controlled and will not be a design constraint.

#### 2.3.2.13 Wind on ~~Mars~~ Surface

The maximum wind velocity on ~~Mars~~ will be 380 ft/sec which will be assumed to act normal to the surface of the solar array.

#### 2.3.2.14 Thermal Environment

The expected thermal environment for the solar panel structure is described in Subsection 2.1.2.

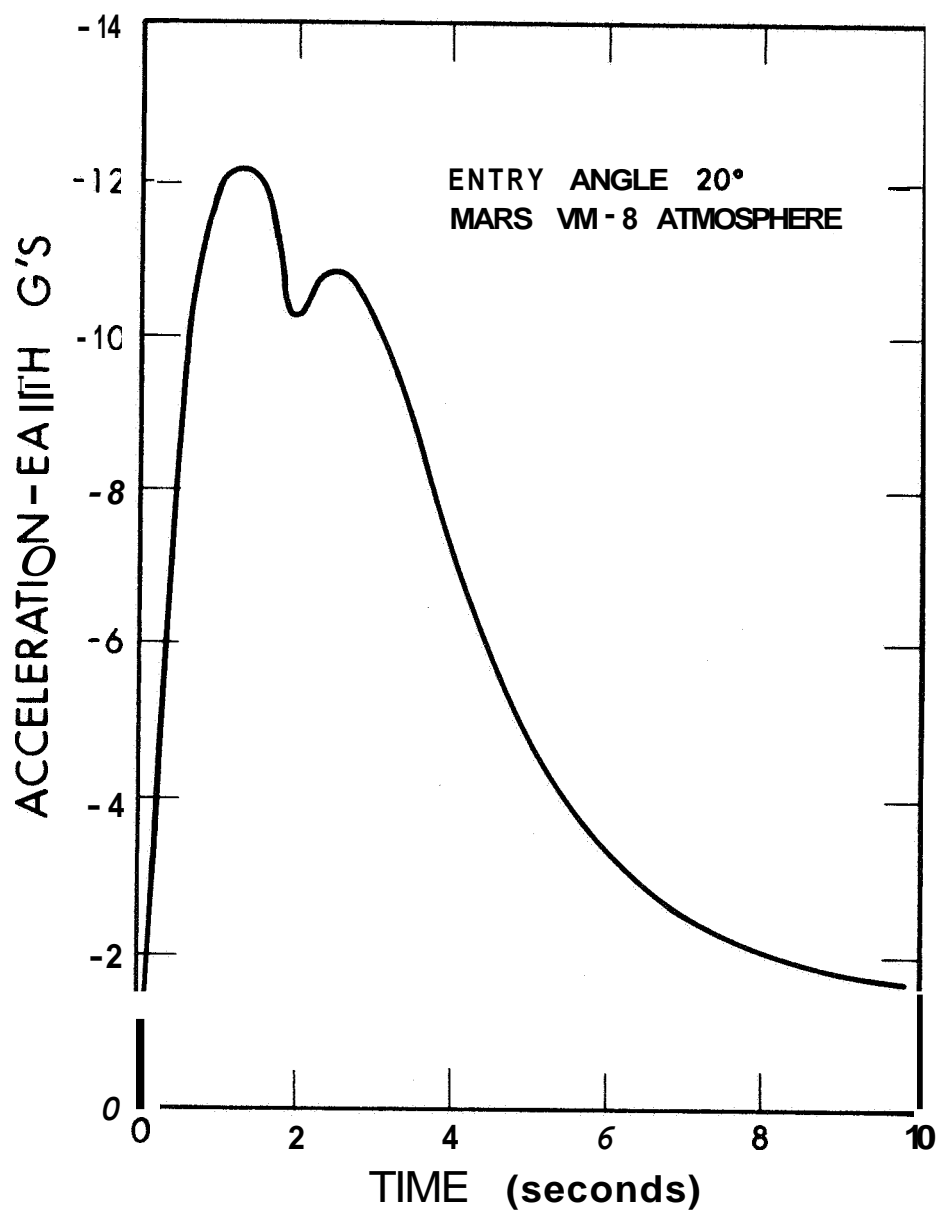


Figure 9. Parachute Opening Shock, JPL Contract 952035

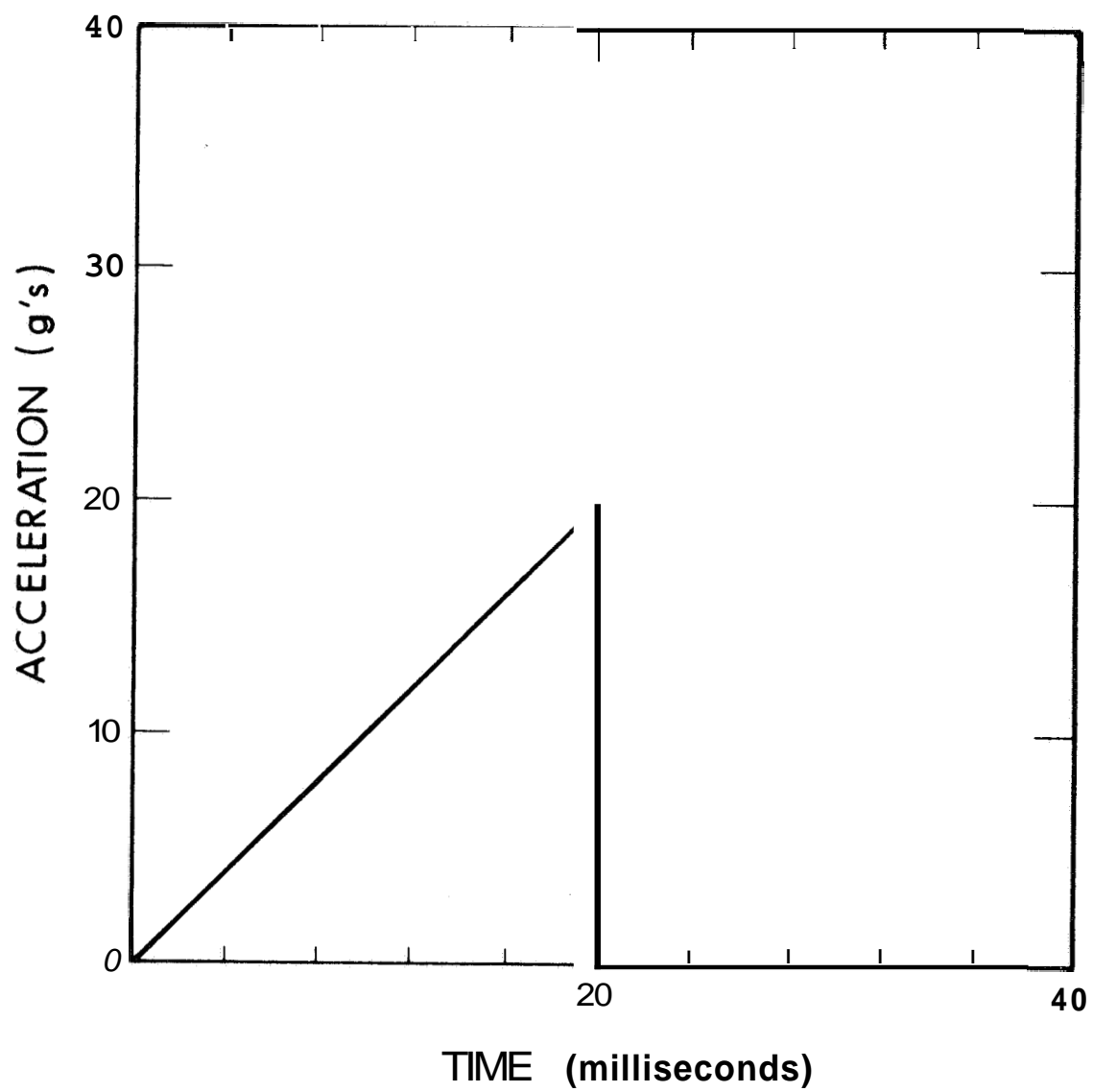


Figure 10. Landing Shock

#### 2.3.2.15 Radiation

The structural materials will be subjected to the radiation environment defined in Subsection 2.1.5 .

#### 2.3.2.16 Corrosive Atmosphere

The ~~Mars~~ atmosphere is 100 percent CO<sub>2</sub>,

### 2.3.3 DESIGN LOADS FOR PRELIMINARY STRUCTURAL ANALYSIS

The induced and natural environments listed in Subsection 2.1 have been reviewed and reduced to a set of critical design loads to be used in trade studies and in preliminary design. The environments which appear to produce the critical design loads are: (1) the random vibration and decaying sinusoids which occur during launch and apply to the stowed configuration of the array, and (2) the wind load on the ~~Mars~~ surface which acts on the deployed array. The environmental conditions will be reassessed as the final designs evolve to determine that these are the critical loading conditions.

#### 2.3.3.1 Design Loads for the Array in the Stowed Configuration

To simplify the preliminary design and analysis procedure, the random vibration and low frequency transients have been reduced to equivalent harmonic inputs. The methods used to determine this equivalence are presented in Subsections 2.3.3.2 and 2.3.3.3. The use of the results is explained in Subsection 2.3.3.4.

### 2.3.3.2 Harmonic Equivalent of Random Vibration Spectrum

The mean square response,  $\overline{\dot{q}^2}$ , of a lightly damped single degree of freedom system to a power spectrum  $w(f)$ , in  $g^2/\text{Hz}$ , is given by Crandall.\*

$$\overline{\dot{q}_r^2} = \frac{\pi}{2} f_n Q W(f_n)$$

where  $f_n$  is the fundamental frequency of the structural element and  $Q$  is the dynamic magnification factor. This result is exact only with infinitely wide band excitation but is a good approximation for the response to a continuous spectrum excitation which is nearly uniform in the neighbourhood of the natural frequency. The  $3\sigma$  response is given by

$$\dot{q}_r = 3 \left( \frac{\pi}{2} f_n Q W(f_n) \right)^{1/2}$$

The probability of a peak exceeding the  $3\sigma$  response is 0.3 percent. The harmonic base excitation  $\ddot{\delta}_s$ , in g's, which produces the  $3\sigma$  response is

$$\ddot{\delta}_s = 3 \left( \frac{\pi}{2} \frac{f_n W(f_n)}{Q} \right)^{1/2}$$

This relation has been evaluated for a frequency range from 10 Hz to 2000 Hz for  $Q$ 's of 20 and 50 and the power spectrum shown in Fig. 8. These results are plotted in Fig. 11.

\*S. H. Crandall, Random Vibration, Technology Press, MIT with Wiley, 1958, pp. 77-90.

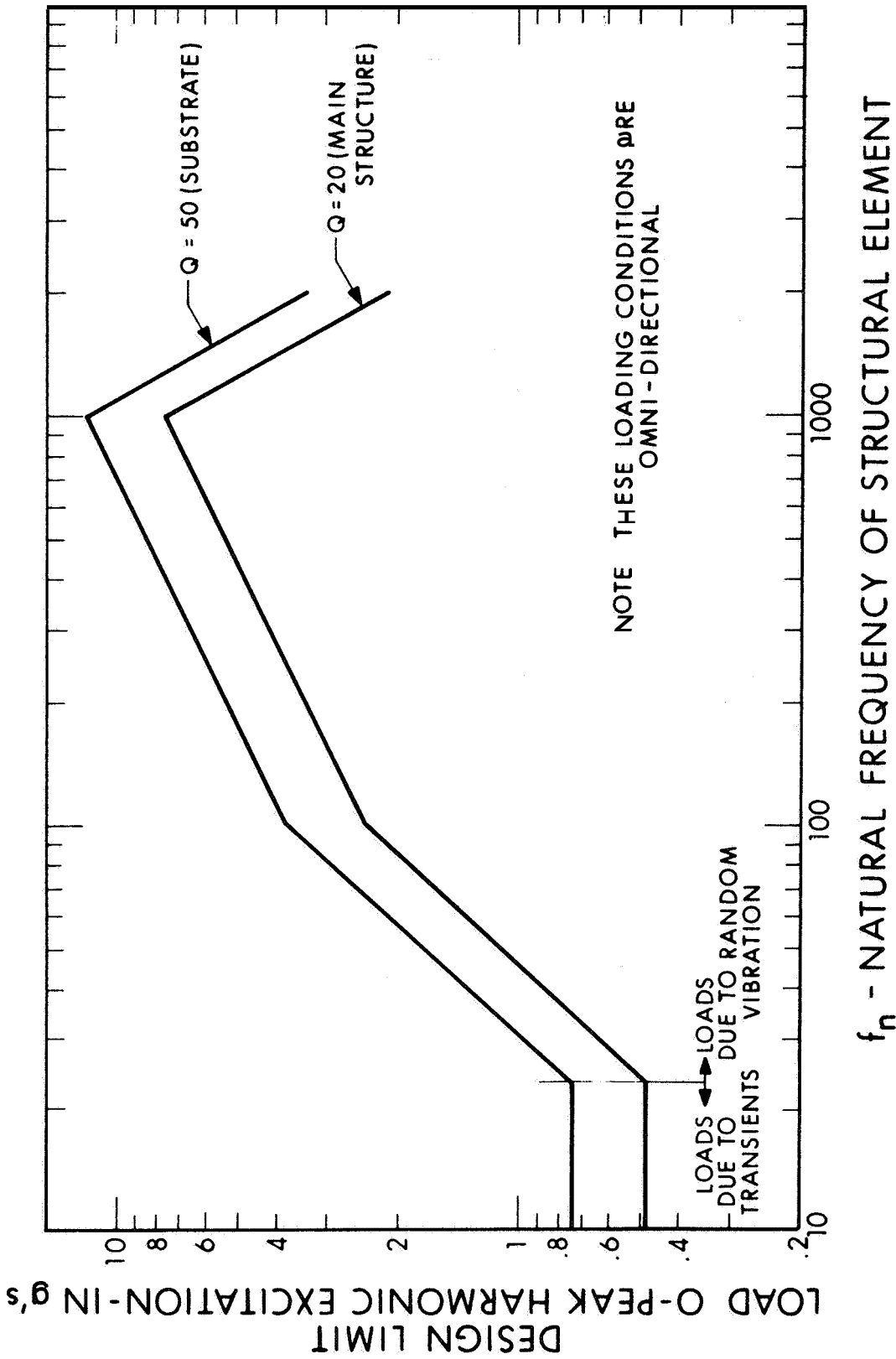


Figure 11. Design Loads for Launch Configuration

### 2.3.3.3 Harmonic Equivalent of Low Frequency Transients

The harmonic base excitation which is equivalent to the low frequency decaying sinusoids was calculated as follows. The response of a simply supported beam to a base excitation defined by

$$\ddot{\delta}_s(t) = 2.1 g e^{-b\omega_n t} \sin \omega_n t$$

$$\text{for } 0 \leq t \leq \frac{40\pi}{\omega_n}$$

$$\text{and } e^{-b\omega_n t} = 0.05 \text{ when } t = \frac{40\pi}{\omega_n}$$

where  $\omega_n$  is the circular natural frequency of beams having dynamic magnification factors of 20 and 50. The maximum dynamic bending moment produced by the decaying sinusoidal excitation was equated to the maximum bending moment produced by harmonic excitation and the magnitude of the equivalent harmonic excitation calculated. The results are plotted in Fig. 11.

### 2.3.3.4 Use of the External Load Curves

The external loads defined in Fig. 11 are designed limit loads which are to be multiplied by 1.25 to get the ultimate design load.

In the design analysis procedure, the structural elements of the solar panel array are to be dynamically decoupled by a separation of their fundamental frequencies. Therefore, the loads to be applied in sizing each element are a function of the fundamental frequency and magnification factor of that element only.



The procedure which is followed is to make a preliminary estimate for the geometry of a structural element and calculate its natural frequency. Then, with the frequency and magnification factor for the element (assumed to be 20 for frame members and 50 for substrate), the equivalent harmonic base excitation may be determined from Fig. 11. The internal loads and deflections for the structural element can then be calculated from the generalized load and deflection curves and relations which have been developed by EOS for this purpose.

If the calculated stresses exceed the allowable stress for the structural element, it may be necessary to deviate from the "minimum weight configuration" for that element based on a nonfrequency-dependent loading condition. That is, if more material is added to provide the necessary strength, it must be added in a manner which does not increase the stiffness (if the natural frequency of the element is above 24 Hz) since the loads increase as the stiffness increases. In short, the weight optimization study of the structure must include the fact that the loads vary as the configuration of the structural element varies.

#### 2.3.3.5 Design Load for Deployed Array on the Martian Surface

For preliminary design purposes, the wind loading on the solar array will be treated as a static load which can be calculated from the relations for stagnation pressure in the flow of a compressible gas. In the final analysis the dynamic loading due to formation of Von Karman vortices will be considered.

#### 2.3.3.6 Calculation of Stagnation Pressure

Assuming the wind is normal to the panel surface, the stagnation pressure,  $P_o$ , is given by

$$P_o = P \left( 1 + \frac{\gamma}{2} \frac{V^2}{a^2} \right)^{\frac{\gamma}{\gamma-1}}$$

where

$$P = \text{static pressure on Mars} = 7 \text{ mb} = 0.135 \text{ psi}$$

$$K = C_p/C_v \text{ (for CO}_2 \text{ at 150}^\circ\text{K)} = 1.28$$

$$M = \text{Mach number} = V/\sqrt{KgRT}$$

$$g = 386 \text{ in./sec}$$

$$V = \text{maximum velocity of Martian wind} = 4560 \text{ in./sec}$$

$$R_{\text{CO}_2} = 35.13 \text{ ft-lb/lb } ^\circ\text{R}$$

$$T = \text{absolute temperature (assume average temperature)} = 225^\circ\text{K} = 405^\circ\text{R}$$

The Mach number is

$$M = V/\sqrt{KgRT}$$

$$M = \frac{4.560}{9.18} = 0.496$$

And the stagnation pressure is

$$P_o = 0.135 \left[ 1 + \frac{1.28-1}{2} (0.496)^2 \right]^{\frac{1.28}{1.28-1.0}}$$

$$P_o = 0.135 [1.034442]^{4.57} = 0.135 [1.15362]$$

$$P_o = 0.155$$

The differential pressure acting on the panel is

$$P_o - P = 0.155 - 0.135 = 0.020 \text{ psi, or } 2.88 \text{ lb/ft}^2$$

### 2.3.3.7 Conclusion

The design load for the deployed panel will be a static pressure of 0.020 psi.

## SECTION 3

### TASK II CONSIDERATIONS

#### 3.1 PRELIMINARY THERMAL ANALYSIS

##### 3.1.1 SOLAR ARRAY THERMAL ENVIRONMENT

The temperature time history of a spacecraft mounted solar panel operating on the surface of Mars is determined by four criteria, which are listed below in decreasing order of influence:

- a. Solar Intensity
- b. Interaction with the surface of Mars
- c. Interaction with the Martian atmosphere
- d. Interaction with the spacecraft

The last two items can be discussed only qualitatively until a preliminary panel design is completed. A representative view factor of the Martian surface and a rough estimate of atmospheric effects were used to generate the preliminary temperature estimates given in the next section. A discussion of the influence of the Martian atmosphere is given below.

The atmosphere was assumed to be 100 percent CO<sub>2</sub> at a pressure of 7 millibars (0.1 psia). This atmosphere has many of the same effects on the landscape of Mars as the Earth's atmosphere has on Earth, with the exception of rain and water erosion. It acts as a temperature equalizer, absorbing heat from the surface during the day and giving it back at night. Changes in density caused by changes in temperature set up local winds which are assumed to average 150 ft/sec with gusts of up to 280 ft/sec. The atmosphere will interact with the spacecraft in the following ways :

- a. It will remove heat by convection during periods of sunlight and add heat at night.
- b. It will carry dust particles and other contaminants.
- c. It will exert wind loads on the exposed surfaces.
- d. It will absorb infrared radiation from spacecraft components.

The heat transfer rates (item a) were investigated by assuming a flat plate parallel to the wind flow. The Reynolds number as a function of flow length along the plate was found to be in the laminar range up to about 4 feet at the average wind velocity of 150 ft/sec. Therefore, laminar flow will predominate over most solar panel and spacecraft configurations for all but the highest wind speeds. The atmospheric pressure at ground level is too high for any rarefied gas effects, such as "slip" flow.

The heat transfer relationship for a flat plate in laminar flow is given below.

$$h = 0.332 \, k/d \, (\text{Re})^{1/2} (\text{Pr})^{1/3}$$

where

$h$  = heat transfer coefficient,  $\text{W/in.}^2 \, ^\circ\text{C}$ ,

$k$  = gas thermal conductivity,  $\text{W/in.}^\circ\text{C}$ ,

$d$  = flow length, in.,

$\text{Re}$  = Reynolds number based on  $d$ ,

$\text{Pr}$  = Prandtl number,

for  $d = 10$  in. at 150 ft/sec wind velocity,

$h = 0.0013 \, \text{W/in.}^2 \, ^\circ\text{C}$ .

This is comparable to still air natural convection rates on Earth and an order of magnitude below wind blown convection on Earth. Similarly, the Martian natural convection rates are an order of magnitude lower; therefore, although wind convection has an appreciable influence on the panel radiation, heat transfer is still the dominant mode.

The effects of dust accumulation cannot as yet be quantitatively assessed. The effects of wind loads are discussed below.

The effects of atmospheric radiation absorption from the spacecraft are estimated in Fig. 12. In this figure, the large absorption band of CO<sub>2</sub> in the 14-16 $\mu$  range was approximated by a simplified model which is shown in the insert. Other higher absorption bands were neglected. Absorption between 14 and 16 microns as a function of source temperature was calculated. The drop below 200°K is not accurate since there are probably absorption bands at longer wavelengths which take care of some low temperature radiation. An adequate engineering estimate of the absorption of the atmosphere at solar panel/spacecraft emission temperatures is 10 percent with a 90 percent transmissivity. This number was used in all calculations.

### 3.1.2 SOLAR PANEL TEMPERATURE

A heat balance was taken on the solar panel temperature extremes under a variety of Martian environmental conditions. The atmospheric effects discussed in the previous section were used. A table of solar panel temperature estimates is given below, and a plot of diurnal temperature variation for one case is shown in Fig. 13. A discussion of the heat balance follows.

<u>Solar Intensity</u>	<u>Surface Temperature</u>	<u>Solar Panel Temp.</u>
50 mW/cm <sup>2</sup>	300°K	* 296.8°K
74 mW/cm <sup>2</sup>	312°K	* 315.3°K
0 (Darkness at aphelion)	150°K	145.7°K
0 (Darkness at perihelion)	211°K	198.4°K

\* These numbers are slightly lower than previously released estimates. The change is due to a correction in  $\alpha_s$  from 0.90 to 0.81.

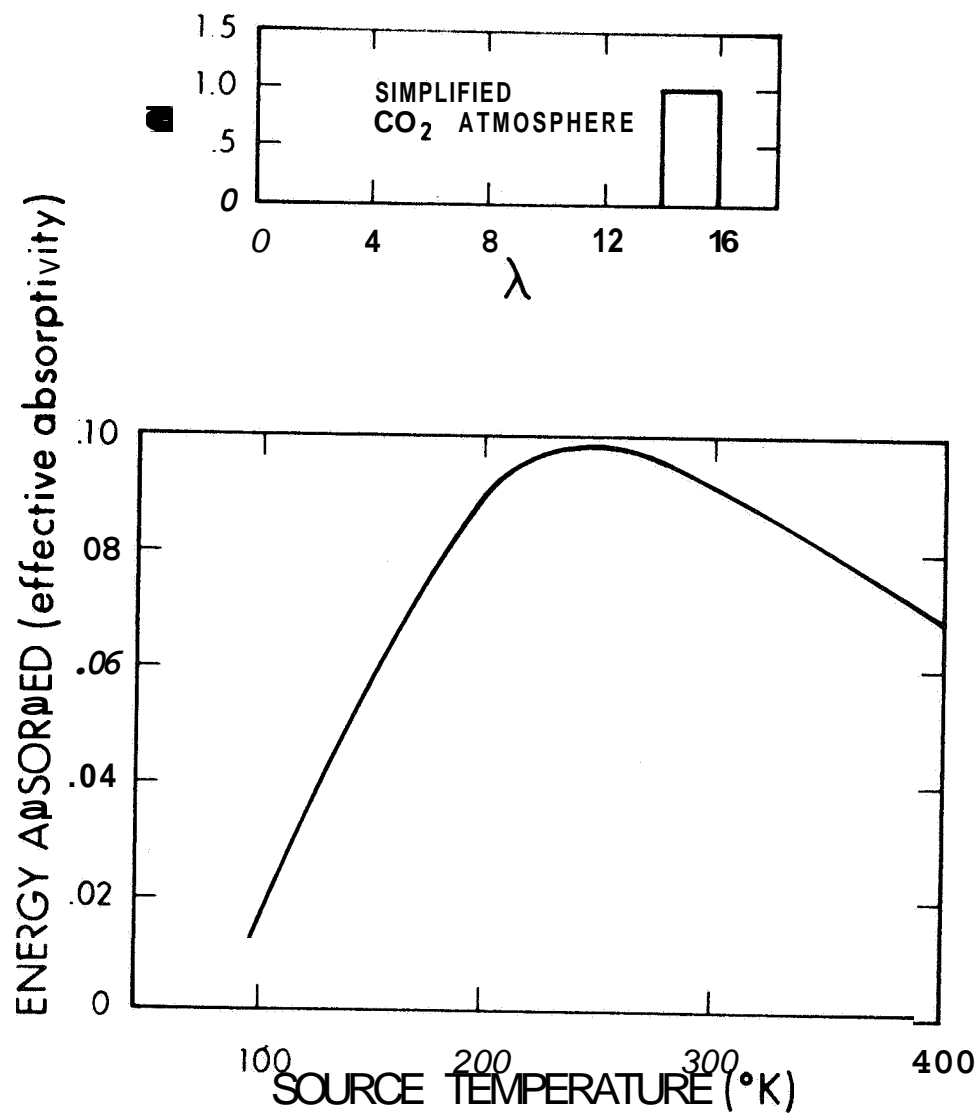


Figure 12. Martian Atmosphere Absorption of Infrared Radiation

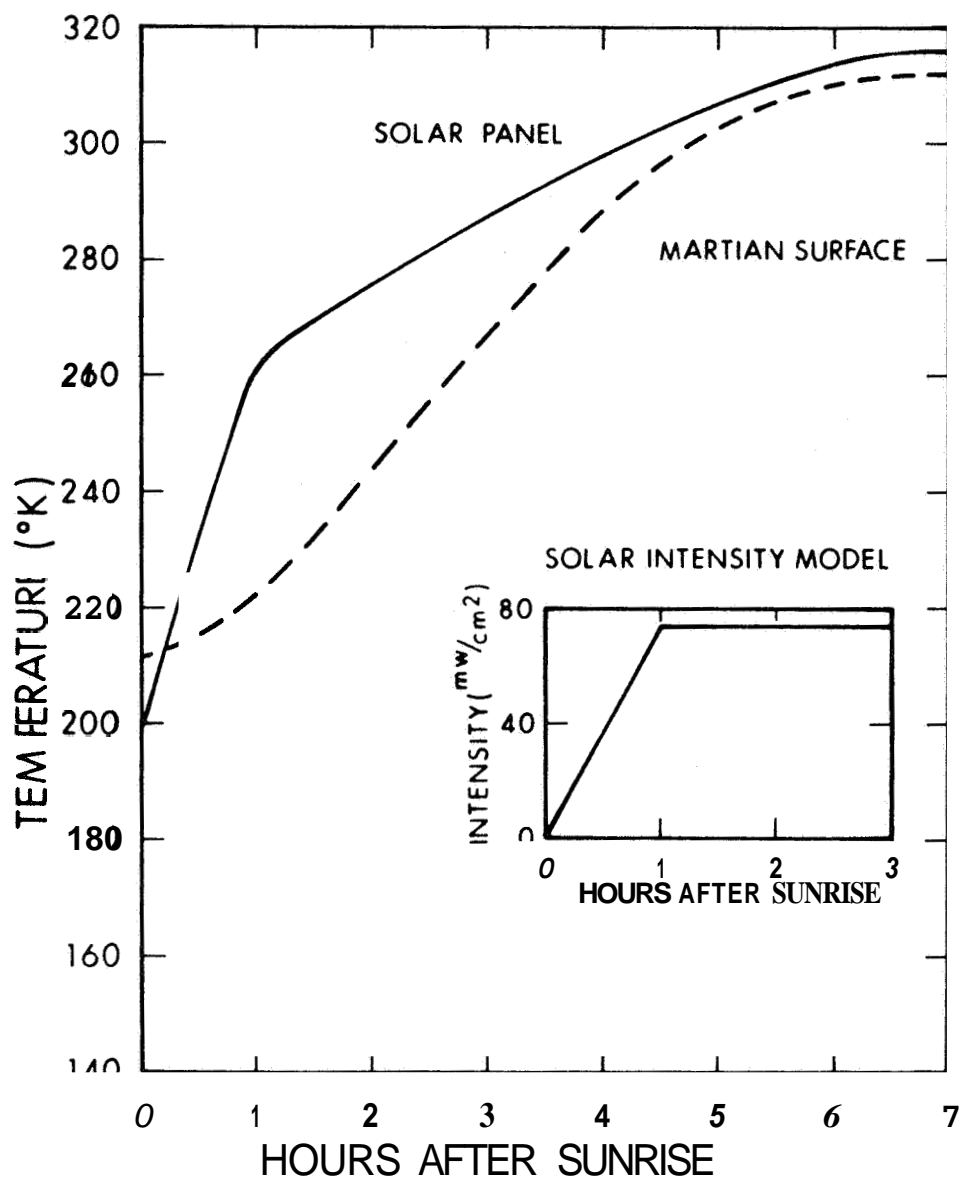


Figure 13. Diurnal Temperature Variation, Equator at Perihelion

#### 3.1.2.1 Heat Balance

In words, for the steady state:

#### 3.1.2.2 Panel Upper Surface

Solar heating = energy converted to electricity + radiation to the atmosphere + radiation to space + convection to the atmosphere + conduction to the panel lower surface.

#### 3.1.2.3 Panel Lower Surface

Conduction from the upper surface = radiation to the surface of Mars + convection to the atmosphere.

Assuming a uniform panel temperature, panel surface area = unity, and combining both equations, in symbols:

$$\begin{aligned} \alpha_s F G_s (1-\eta) &= t \epsilon \sigma T_1^4 \\ &+ (1-t) \epsilon (\sigma T_1^4 - \sigma T_a^4) - 2h (T_1 - T_m) \\ &+ \epsilon (\sigma T_1^4 - \sigma T_m^4) \end{aligned}$$

where

$\alpha_s$  = solar absorptivity of panel = 0.81  
 $F$  = atmospheric attenuation of sunlight = 0.92  
 $G_s$  = solar constant at Mars  
 $\eta$  = solar panel efficiency  
 $t$  = atmospheric transmissivity to Mars radiation  
 $\epsilon$  = solar panel emissivity = 0.85 (both sides)  
 $\sigma$  = Boltzmann's constant,  $36.6 \times 10^{-12}$  watts/in<sup>2</sup> °K  
 $T_1$  = average panel temperature, °K



$T_a$  = Mars sky temperature,  $230^{\circ}\text{K}$   
 $h$  = heat transfer coefficient,  $\text{watts/in}^2 \text{ }^{\circ}\text{K}$   
 $T_m$  = atmospheric temperature and Mars surface temperature,  
 $^{\circ}\text{K}$

The equation was solved for the cases listed above. In addition, a transient case was solved assuming a panel weight of  $0.5 \text{ lb/ft}^2$  and an average specific heat of  $0.2 \text{ Btu/lb }^{\circ}\text{F}$ . This is plotted for the first 7 hours after sunrise in Fig. 13. The large difference between planetary and panel temperatures after the first hour has a considerable leveling effect. In all cases, the atmosphere and surface temperatures were assumed to be equal, since there is no rational basis for assigning a lead or lag during the day.

## 3.2 PRELIMINARY POWER ANALYSIS

### 3.2.1 RADIATION ENVIRONMENT AND EFFECTS

There are two basic types of radiation the solar array may encounter on the Martian surface, proton radiation from solar flares, and ultra-violet radiation. The galactic cosmic radiation near Mars consists of essentially the proton component and its secondary radiation produced in the Martian atmosphere.

The intensity of the solar flares for the planetary array mission in 1973 is based on the information provided in the JPL Voyager Environmental Predictions Document SE003BB01-1B28. The energy distribution of solar flare radiation is based on the power law obtained from Section V of the referenced JPL document.

$$I = KE^{-n} \quad (1)$$

where

$$\begin{aligned} I &= \text{the solar flare intensity in protons/cm}^2\text{-time} = \phi \\ E &= \text{proton energy, MeV} \\ K &= \text{constant} = 2.47 \times 10^8 \\ n &= \text{constant} = 0.189 \end{aligned}$$

Based on the table presented in Section IV, D.4 of the JPL document,  $I = 2.47 \times 10^8 E^{-0.189}$  protons/cm<sup>2</sup>-year for 1973, at the Martian surface. The proton radiation degrades the cover glass and the solar cells. The basic radiation effect on cover glass is a transmission loss from discoloration. This discoloration is caused by the formation of 'F' centers. Some discoloration is also noted in fused silica (quartz), but it is much worse in microsheet (soda-lime glass) due to the increased impurities found in the glass. Radiation has little or no effect on the physical strength of the filter glass.

The basic mechanism that causes the degrading of the cells is the formation of recombination centers in the bulk material of the solar cell. As a result of these new recombination centers, the holes and electrons that are generated by the photons recombine before reaching the N-P junction. This electrical energy is essentially lost as far as useful output is concerned. The overall effect of proton radiation on solar cells is the decreasing of the effective current.

The effect of radiation on solar cells is determined by the radiation degradation equation:

$$Q = \left[ 7/9 \left( \frac{\phi}{\phi_c} \right)^{1/2} \right] \quad (2)$$

where

Q = percent of power capability remaining after bombardment with integrated flux,  $\phi$

Q<sub>c</sub> = "critical" flux necessary to produce a 25 percent degradation of solar cell output power. (In this case:  $\phi_c = 1 \times 10^{11}$  protons/cm<sup>2</sup>.)

The above equation was developed by a member of the technical staff at EOS based on the theoretical and empirical considerations of radiation induced damage in silicon solar cells. The range of protons through three mil filters is approximately 3 MeV which gives a proton flux of  $2.0 \times 10^8$  p/cm<sup>2</sup>-year, using Eq. 1. This flux gives a radiation degradation of 1.7 using Eq. 2.

### 3.2.2 PRELIMINARY

In order to calculate a power analysis for the planetary solar array, a number of basic assumptions must be made with respect to the circuit requirements of the array.

Cell type - 2 x 2 cm (1-3  $\Omega$ cm)

Cell output at STD AMO conditions - 27°C

1) 0.012 THK - 60 mW @ 450 mV

2) 0.008 THK - 55 mW @ 450 mV

3) 0.004 THK - 47 mW @ 450 mV

Circuit voltage - 28.0 volts

No. of cells in parallel/circuit - 6

The following values are given as derived and shown earlier in this report and represent worst case conditions.

Solar irradiance -  $50 \text{ mV/cm}^2$   
 Atmospheric loss - 8%  
 Surface irradiance -  $46 \text{ mW/cm}^2$   
 Panel temperature -  $300^\circ\text{K}$  ( $27^\circ\text{C}$ )  
 Radiation degradation @ one year - 4%

The following calculation is given to derive the minimum square footage required to produce 200 watts of electrical power on Mars at solar noon,

- a. Current/cell @ maximum power point:
  - 1)  $0.021 - 60/450 = 133.2 \text{ mA}$
  - 2)  $0.008 - 55/450 = 122.2 \text{ mA}$
  - 3)  $0.004 - 47/450 = 104.5 \text{ mA}$
- b. Correction for solar irradiance  $46/140 = .33$  factor
  - 1)  $0.012 - 133.2 (.33) = 43.8 \text{ mA @ } 450 \text{ mV}$
  - 2)  $0.008 - 122.2 (.33) = 40.2 \text{ mA @ } 450 \text{ mV}$
  - 3)  $0.004 - 104.5 (.33) = 34.5 \text{ mA @ } 450 \text{ mV}$
- c. Correction for filter and fabrication losses (5%)
  - 1)  $0.012 - 43.8 (.95) = 41.6 \text{ mA}$
  - 2)  $0.008 - 40.2 (.95) = 38.2 \text{ mA}$
  - 3)  $0.004 - 34.5 (.95) = 32.8 \text{ mA}$
- d. Correction for one year radiation degradation (2%)
  - 1)  $0.012 - 41.6 (.98) = 40.8 \text{ mA (18.36 mW/cell)}$
  - 2)  $0.008 - 38.2 (.98) = 37.4 \text{ mA (16.83 mW/cell)}$
  - 3)  $0.004 - 32.8 (.98) = 32.1 \text{ mA (14.44 mW/cell)}$
- e. Number of cells in series, adding 1 volt for diode and wiring loss:
 
$$28.0 + 1.0 = 29.0 / .450 = 64.5 \text{ (65 cells)}$$

Operating voltage/cell = 446 mV

f. Current/Array:

$$200\text{W}/28.0\text{V} = 7.15\text{A}$$

g. Number of cells in parallel/array:

$$1) \ 0.012 - 7.15/.0408 = 176$$

$$2) \ 0.008 - 7.15/.0374 = 191$$

$$3) \ 0.004 - 7.15/.0321 = 223$$

h. Number of six cell circuits/array:

$$1) \ 0.012 - 179/6 = 29.4 \ (30)$$

$$2) \ 0.008 - 196/6 = 31.9 \ (32)$$

$$3) \ 0.004 - 227/6 = 37.2 \ (38)$$

i. Number of total cells/array:

$$1) \ 0.012 - 30 \ (6) \ (65) = 11,700$$

$$2) \ 0.008 - 32 \ (6) \ (65) = 12,480$$

$$3) \ 0.004 - 38 \ (6) \ (65) = 14,820$$

j. Watts output of total array:

$$1) \ 0.012 - 18.36 \ (11,700) = 214.8\text{W}$$

$$2) \ 0.008 - 16.83 \ (12,480) = 210.0\text{W}$$

$$3) \ 0.004 - 14.44 \ (14,800) = 214.0\text{W}$$

k. Area of cell

$$0.793 \times 0.793 = 0.63 \text{ in.}^2$$

1. Assuming a 90 percent packing factor the minimum area of the array would be:

$$1) \ 0.012 - 0.63 \ (1.11) \ (11,700) = 8,182 \text{ in.}^2 - 56.8 \text{ ft}^2$$

$$2) \ 0.008 - 0.63 \ (1.11) \ (12,480) = 8,730 \text{ in.}^2 - 60.6 \text{ ft}^2$$

$$3) \ 0.004 - 0.63 \ (1.11) \ (14,820) = 10,380 \text{ in.}^2 - 72.0 \text{ ft}^2$$

The following calculation is given to derive specific wt/ft<sup>2</sup> of the solar array:

a. Weight analysis, less substrate:

Cell thickness, inch	0.012	0.008	0.004
Cell weight, solderless (g)	0.29	0.20	0.11
Filter weight, 0.003 thick (g)	0.10	0.10	0.10
Filter adhesive (g)	0.03	0.03	0.03
Connector and boss/cell (g)	0.10	0.10	0.10
Mounting adhesive (g)	<u>0.05</u>	<u>0.05</u>	<u>0.05</u>
Total (g/cell)	0.57	0.48	0.39
Total g/ft <sup>2</sup> (206 cells/ft <sup>2</sup> )	117.4	98.9	80.3
Total lbs/ft <sup>2</sup>	0.259	0.218	0.177

b. Earth AMO power of the array:

$$200 \text{ W}/0.33 = 606 \text{ W}$$

c. Maximum design weight of array:

JPL specified 20 W/lb

$$606/20 = 30.3 \text{ lb}$$

d. Assuming 1/3 of the allowable weight for deployment structure, and 2/3 for array structure the allowable lbs/ft<sup>2</sup> of the array including cells are:

- 1)  $0.012 - 20.2/56.8 = 0.358 \text{ lbs/ft}^2$
- 2)  $0.008 - 20.2/60.6 = 0.333 \text{ lbs/ft}^2$
- 3)  $0.004 - 20.2/72.0 = 0.281 \text{ lbs/ft}^2$

e. Allowable lbs/ft<sup>2</sup> for substrate:

- 1)  $0.012 - 0.358 - 0.259 = 0.099 \text{ lbs/ft}^2$
- 2)  $0.008 - 0.333 - 0.218 = 0.115 \text{ lbs/ft}^2$
- 3)  $0.004 - 0.281 - 0.177 = 0.104 \text{ lbs/ft}^2$

f. Specific power/area:

$$1) \quad 0.012 - 214.8/56.8 = 3.78 \text{ W/ft}^2 \text{ (11.5 W/ft}^2, \text{ AMO)}$$

$$2) \quad 0.008 - 210.0/60.6 = 3.46 \text{ W/ft}^2 \text{ (10.5 W/ft}^2, \text{ AMO)}$$

$$3) \quad 0.004 - 214.0/72.0 = 2.97 \text{ W/ft}^2 \text{ (9.0 W/ft}^2, \text{ AMO)}$$

The thinner cells, though lighter, require a larger panel area due to their lower specific power output. This calculation is based on a fixed legislated value of 20 W/lb at Earth AMO. It has been shown that the tradeoff of lighter cell weight vs larger panel area is essentially equal providing a substrate weight of approximately  $0.10 \text{ lb/ft}^2$  can be met. A slight advantage can be gained by using the 0.008 thick solar cells, if it would be advantageous for substrate weight allowance. The advantage, all aspects considered, however, lies with the thicker cells, as they will require a 21 percent smaller panel which is less costly, easier to deploy and support in the wind conditions on Mars.

### 3.3 DISCUSSION OF POSSIBLE ARRAY CONCEPTS

In Subsection 3.2 a minimum array size was outlined as follows:

a. Area -  $56.8 \text{ ft}^2$

b. Weight - 20.2 lb

This array area is defined as the minimum panel size with 0.012 thick cells at a 90 percent packing factor, at an array temperature of  $300^\circ\text{K}$ , and with the array normal to the noon sun with no shadow losses.

In analyzing the possible array concepts which may be utilized for a Martian solar array, the first area of consideration covers the orientation modes. The orientation considerations are that the array must have the inherent capability, or be able to be positioned in such a way as to account for the following environmental factors:

- a. Latitude of spacecraft after landing
- b. Seasonal changes of sun angle
- c. Slope of terrain upon which the spacecraft has landed

An additional factor that must be considered is the effect upon the solar array caused by the position of the spacecraft with respect to the plane of the sun's ecliptic. The position of the spacecraft is uncontrolled, and after landing cannot be corrected to a preferred attitude. The effect upon the array will be varied dependent upon the orientation capability of the design.

The various orientation modes considered in the conceptual analysis are depicted in EOS Dwg. 7254-101 (Fig. 14). These are:

- a. Fixed array
- b. Single-axis orientation
- c. Two-axis orientation
- d. Three-axis orientation

It is also important to note that the orientation analysis presented does not indicate a preference for a structural design of the solar array. The actual array substrate, rollup, semirigid, or rigid, will have essentially the same limiting factors with respect to a suntime envelope.

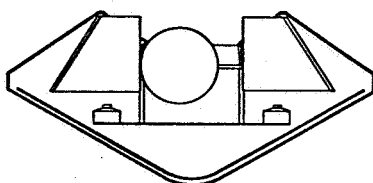
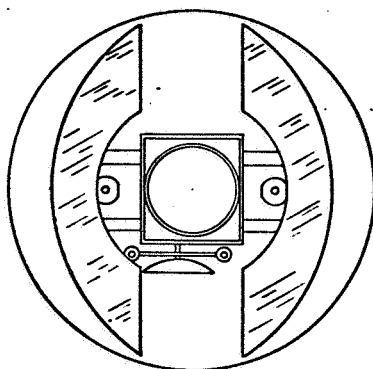
The preliminary orientation analysis as shown in Fig. 14 is actually a tradeoff study of the anticipated area and weight required to provide a projected area of 56.8 sq ft of solar array for the different orientation modes shown. In addition, an estimated 12 hr power profile is shown considering that the array has been oriented to its best case condition for worst case environmental conditions.

Certain of the orientation modes, primarily 5 and 6, could be readily adapted to continuous sun tracking, to provide a nearly uniform power profile.

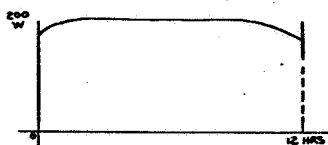


SECURITY CLASSIFICATION

NOTES



FIXED ARRAY  
CONFIGURATION 1



POWER PROFILE (DAILY)

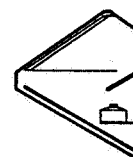
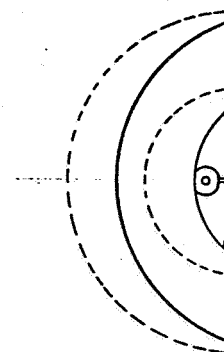
AREA : 171 SQ FT  
WEIGHT : 61 LBS

ADVANTAGES:

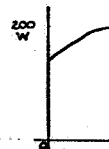
1. NEARLY UNIFORM POWER PROFILE.
2. NOT DEPENDENT UPON VEHICLE ATTITUDE.
3. ELIMINATES SHADOW PROBLEM.
4. MINIMUM STRUCTURAL BRACING.
5. NO DEPLOYMENT MECHANISMS.
6. NO ORIENTATION MECHANISMS.
7. HIGH RELIABILITY DUE TO SIMPLICITY.
8. MEETS ALL REQUIREMENTS EXCEPT TOTAL WEIGHT.
9. NO APPARENT WIND LOADING PROBLEM.

DISADVANTAGES:

1. OVER DESIGN GOAL WEIGHT BY APPROX 2% FACTOR.
2. REQUIRES 3% NUMBER OF SOLAR CELLS BASED ON MINIMUM SOLAR ARRAY.
3. COMPLEX PANEL SHAPE.



MODIF  
CONI



AREA : 171 SQ FT  
WEIGHT : 66 LBS

ADVANTAGES:

1. NEARLY UNIFORM POWER.
2. NOT DEPENDENT UPON VEHICLE ATTITUDE.
3. ELIMINATES SHADOW PROBLEM.
4. NO ORIENTATION MECHANISMS.
5. HIGH RELIABILITY DUE TO SIMPLICITY.
6. MEETS ALL REQUIREMENTS EXCEPT TOTAL WEIGHT.
7. NO APPARENT WIND LOADING PROBLEM.

DISADVANTAGES:

1. OVER DESIGN GOAL WEIGHT BY APPROX 2% FACTOR.
2. REQUIRES 3% NUMBER OF SOLAR CELLS BASED ON MINIMUM SOLAR ARRAY.
3. REQUIRES SINGLE ACTION MECHANISMS.
4. REQUIRES COMPLEX STRUCTURE.
5. MODERATELY COMPLEX.

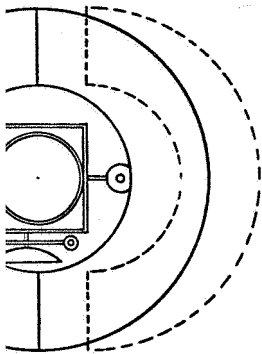
7254-Q-1

16

15

14

13



FIXED ARRAY

CONFIGURATION 2

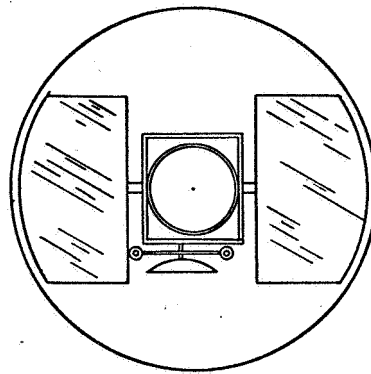


POWER PROFILE (DAILY)

POOR PROFILE.  
VEHICLE ATTITUDE.  
SIMPLE.  
SIMPLICITY.  
EXCEPT TOTAL WEIGHT.  
PROBLEM.

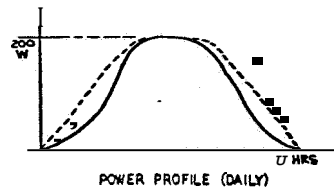
BY APPROX. 2X FACTOR.  
SOLAR CELLS BASED

DEPLOYMENT MECHANISM.  
STRUCTURAL BRACING.  
PANEL CONFIGURATION.



SINGLE AXIS ORIENTATION

CONFIGURATION 3



POWER PROFILE (DAILY)

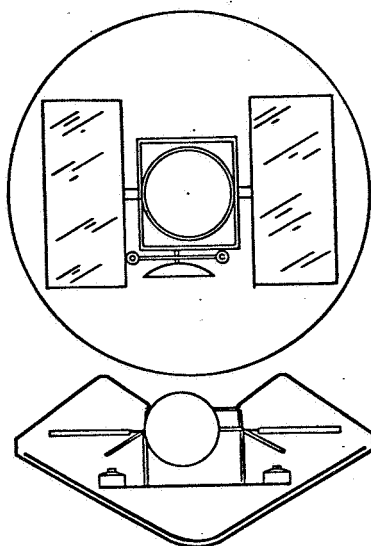
AR : 114 SQ FT  
WEIGHT: 50 LBS

ADVANTAGES:

1. REQUIRES ONLY SINGLE AXIS ORIENTATION MECHANISM.
2. SIMPLE PANEL CONFIGURATION WITH THE EXCEPTION OF SIZE.

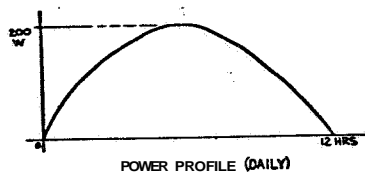
DISADVANTAGES:

1. POOR POWER PROFILE.
2. EFFICIENCY IS DIRECTLY DEPENDENT UPON VEHICLE ATTITUDE.
3. HAS SHADOW PROBLEM.
4. MAY REQUIRE DEPLOYMENT MECHANISM.
5. REQUIRES 2X NUMBER OF SOLAR CELLS BASED ON MINIMUM SOLAR ARRAY.
6. LARGE PANEL AREA WOULD REQUIRE HEAVIER STRUCTURAL BRACING.
7. OVER DESIGN GOAL WEIGHT BY APPROX 1.6X FACTOR.
8. MAXIMUM WIND LOADING PROBLEM DUE TO PANEL SIZE.



TWO AXIS ORIENTATION

CONFIGURATION 4



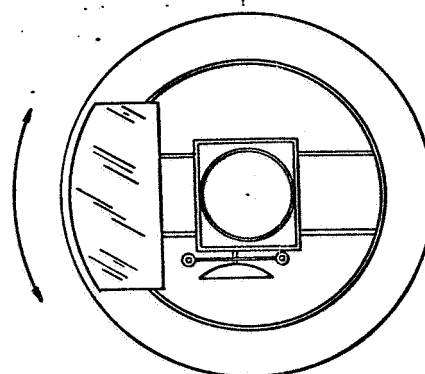
AREA: 85 SQ FT  
WEIGHT: 44 LBS

ADVANTAGES:

1. IMPROVED POWER PROFILE BASED ON SINGLE AXIS ORIENTATION
2. SIMPLE PANEL CONFIGURATION, EXCEPT FOR SIZE.

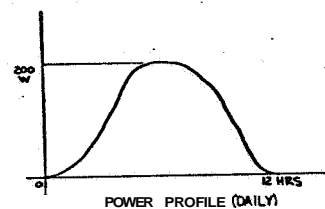
DISADVANTAGES:

1. EFFICIENCY DEPENDENT UPON VEHICLE ATTITUDE.
2. HAS SHADOW PROBLEM.
3. MAY REQUIRE DEPLOYMENT MECHANISM.
4. REQUIRES APPROXIMATELY 1.5X NUMBERS OF SOLAR CELLS BASED UPON MINIMUM SOLAR ARRAY.
5. OVER DESIGN GOAL WEIGHT BY APPROX. 1.45X FACTOR.
6. REQUIRES 2 AXIS ORIENTATION MECHANISMS.
7. POSSIBILITY RELIABILITY PROBLEM DUE TO TWO AXIS ORIENTATION.



THREE AXIS ORIENTATION

CONFIGURATION 5



AREA: 57 SQ FT  
WEIGHT: 40 LBS

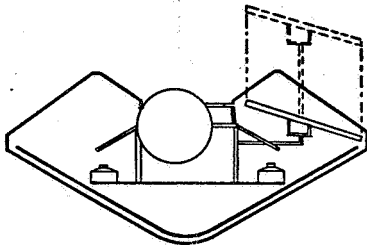
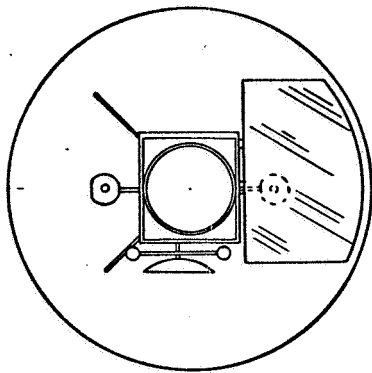
ADVANTAGES:

1. REQUIRES ONE SOLAR PANEL OF MINIMUM AREA.
2. SIMPLE PANEL CONFIGURATION.
3. HAS NO SHADOW PROBLEM.
4. NOT DEPENDENT UPON VEHICLE ATTITUDE.
5. HAS MINIMUM WIND LOADING PROBLEM.

DISADVANTAGES:

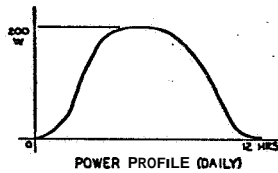
1. REQUIRES 3 AXIS ORIENTATION MECHANISM.
2. REQUIRES POSSIBLE DEPLOYMENT MECHANISM.
3. VIOLATES JPL GROUND RULE OF NON-USABLE SPACE AREA ON VEHICLE.
4. OVER DESIGN GOAL WEIGHT DUE TO 3RD AXIS ORIENTATION MECHANISM BY APPROX 1.3X FACTOR.
5. REQUIRES COMPLICATED ELECTRICAL POWER WIRING.
6. HAS COSINE POWER CURVE PROFILE.

REVISIONS			
ZONE	LTR	DESCRIPTION	DATE



MODIFIED 2 AXIS ERECTED PANEL

CONFIGURATION G



AREA: 57 SQ FT  
WEIGHT: 31 LBS

#### ADVANTAGES

1. REQUIRES ONE SOLAR PANEL OF MINIMUM AREA.
2. SIMPLE PANEL CONFIGURATION.
3. HAS NO SHADOW EFFECT.
4. NOT DEPENDENT UPON VEHICLE ATTITUDE.
5. MEETS ALL JPL REQUIREMENTS, INCLUDING WEIGHT.
6. REQUIRES 2 AXIS ORIENTATION TO EFFECT 3 AXIS CAPABILITY.

#### DISADVANTAGES

1. REQUIRES COMPLICATED DEPLOYMENT & ERECTING MECHANISM.
2. REQUIRES INTEGRATION WITH ANTENNA SYSTEM OF SPACE CRAFT.
3. POSSIBLE WIND LOADING PROBLEM.
4. POSSIBLE RELIABILITY PROBLEM DUE TO COMPLICATED DEPLOYMENT & ERECTING MECHANISM.
5. HAS COSINE POWER CURVE PROFILE.

QTY REQD	SYM	CODE IDENT	PART OR IDENTIFYING NO.	NOMENCLATURE OR DESCRIPTION	MATERIAL	SPECIFICATION	UNIT WT.	ZONE	ITEM NO.
LIST OF MATERIALS									
UNLESS OTHERWISE NOTED LINEAR DIMS. IN INCHES TOLERANCES DECIMAL FRACTION ANGULAR DO NOT SCALE				CONTRACT NO. _____ DRAWN BY <i>M. W. W.</i> DATE _____ CHECKED BY <i>M. W. W.</i> DESIGN BY <i>M. W. W.</i> MATERIAL _____ MPPL _____ TREATMENT/FINISH _____ DESIGN ACTIVITY APPD _____ SIMILAR TO _____ ALT. WT. CALC. WT. _____ CUSTOMER _____					
ON THRU PART NEXT/FINAL NEXT ASSY USED ON				ELECTRO-OPTICAL SYSTEMS, INC. A Subsidiary of Kolls Corporation 300 N. Hollywood St., Pasadena, California, 91107 TITLE ARRAY CONCEPTS (STOWED POSITION)					
EFFECTIVE SERIAL NO. PER ASSY				DWG NO. 12705 U/WG NO. 7254-101 SCALE _____ RELEASE DATE _____ SHEET _____					
USAGE DATA				DRAWING LEVEL					

Figure 14.

50-4

### 3.4 ASPECTS OF MARTIAN ENVIRONMENTAL EFFECTS ON MATERIAL SELECTION

This section discusses certain aspects of the Mars environment which may influence the choice of material or the method of integration of the solar array. The three areas of primary concern are: (1) the effect of carbon dioxide atmosphere which could possibly cause material corrosion, (2) the effect of dust particles on the electrical performance of the array, and (3) the effect of surface pitting on thermal control surface conceivably brought about by dust storms caused by periodic occurrence of high speed wind.

It should be emphasized that the order of magnitude of these effects presented **will** be quite speculative, since available data of Mars environment contain a large degree of uncertainty. The indicated magnitude, however, can be used as a guide in screening out materials or to provide rationale for the array design.

#### 3.4.1 EFFECT OF CO<sub>2</sub> ATMOSPHERE

The atmospheric model selected as the most probable suggests that the Martian atmosphere consists of approximately 100 percent carbon dioxide. The likely mode of CO<sub>2</sub> attack on material at the temperature of 300°K will probably be in the form of weak carbonic acid formed by the combination of CO<sub>2</sub> gas and water vapor. The first order of analysis is to determine the carbon dioxide concentration at Mars surface in comparison to that which exists on Earth.

The Earth atmospheric composition applicable from 0 to 90 km altitude is the following:

	<u>Content</u> (w/o)
N <sub>2</sub>	75.5
O <sub>2</sub>	23.1
A	1.33
CO <sub>2</sub>	0.045
Others in trace amounts	0.005

The number of CO<sub>2</sub> gas molecules in 1 cm<sup>3</sup> of air can be calculated from

$$N_{\text{earth}} = \frac{N_o F \rho_{\text{atm}}}{M}$$

where

$$\begin{aligned}
 N_{\text{earth}} &= \text{CO}_2 \text{ gas molecules/cm}^3 \\
 N_o &= \text{Avogadro number} = 6.02 \times 10^{23} \\
 F &= \text{percent abundance} \\
 \rho_{\text{atm}} &= \text{atmospheric density} = 11.66 \times 10^{-4} \text{ gm/cm}^3 \\
 M &= \text{molecular weight of CO}_2 = 44 \\
 N_{\text{earth}} &= 6.02 \times 10^{23} \times 0.045 \times 10^{-2} \times \frac{11.66 \times 10^{-4}}{44} \\
 &= 9.54 \times 10^{15} \text{ cm}^{-3}
 \end{aligned}$$

For the case of Mars, the abundance is 100 percent and the density is  $1.85 \times 10^{-5} \text{ gm/cm}^3$ . This yields

$$52 \times 10^{17} \text{ cm}^{-3}$$

$$\frac{N_{\text{Mars}}}{N_{\text{Earth}}} = 26.4$$

The result of the above simplified analysis indicates that the CO<sub>2</sub> concentration at Mars is approximately 25 times that on Earth. However, this result should be tempered by the fact that the water vapor content at Mars is one or two orders of magnitude of that on Earth. The net result will be that the degree of attack on material will be negligible such as is experienced on Earth.

It is pertinent to note that several nuclear reactor installations in Britain (such as the Calder Hall reactors) use carbon dioxide as the coolant at high temperatures. These reactors have been in operation for several years and are still operating with no apparent problem in regard to CO<sub>2</sub> attack on material such as stainless steel.

#### 3.4.2 EFFECT OF DUST PARTICLES ON ELECTRICAL PERFORMANCE OF ARRAY

Dust particles which have a range of 1 to 1000 $\mu$  can be made airborne when speed exceeds 300 ft/sec. Such a wind speed is not a normal occurrence but could conceivably exist on a transient basis. Once airborne, the settling dust may affect the electrical performance in two ways. One is to degrade the optical properties of the solar cell cover glass, and second effect will be to create a short circuit condition between two solar cells.

Reduction of solar array output by dust shadowing (optical properties degradation) is not catastrophic and the problem can be solved by mechanical means. Movement of the solar panel, provision of wipers or blowing gas jets are possibilities. In fact, if the tradeoff study proves it to be advantageous, daily solar tracking will provide an automatic means of dust disposal.

The electrical shorting, however, can be catastrophic. Whether or not this is a serious problem depends on the electrical properties of the dust particles. A polarization study of light from the bright or

so-called "desert" regions of Mars suggests the surface to be that of limonite (hydrous ferric oxide). Kuiper, on the other hand, concluded from his infrared studies that the bright areas consist of igneous rock, similar to felsite. Other investigators have found similarity between the polarization curves for Mars and those for volcanic ash and red sandstone. Grains are apt to be coated with an oxide, for example limonite or hematite, which would **mask** the silicate emission spectra. The possible existence of limonite as dust particles can be quite a problem, since it is a relatively good conductor. The electrical resistivity of iron oxide in comparison with other known insulators is as shown below.

<u>Material</u>	<u>Elect. Resistivity (ohm-em) at 300°K</u>
99.24 Fe <sub>2</sub> O <sub>3</sub> and 0.76 TiO <sub>2</sub>	2
99.85 Fe <sub>2</sub> O <sub>3</sub> and 0.15 TiO <sub>2</sub>	60
BeO	
Al <sub>2</sub> O <sub>3</sub>	>10 <sup>13</sup>
H-film (Kapton)	10 <sup>14</sup>

The above discussion suggests strongly that all exposed electrical surfaces should be avoided. This factor should be considered in the specification of solar panel fabrication. One possible solution is, as a final step, to spray a dielectric coating on the panel to prevent the short circuit. However, the optical properties of the cover glass may be compromised. LMSC recently reported a research-type coating which could be used in place of the cover glass. It is unlikely that such a coating will be state-of-the-art by 1969, but is a possibility for a later mission.



### 3.4.3 EFFECT OF DUST STORM ON SURFACE

According to the probable atmospheric model (VM-2), the normal continuous wind speed on Martian surface (from 0 to 10 meters height) is 150 ft/sec. The corresponding surface maximum speed is 380 ft/sec. This latter speed may be as high as 450 ft/sec if the VM-8 model is considered.

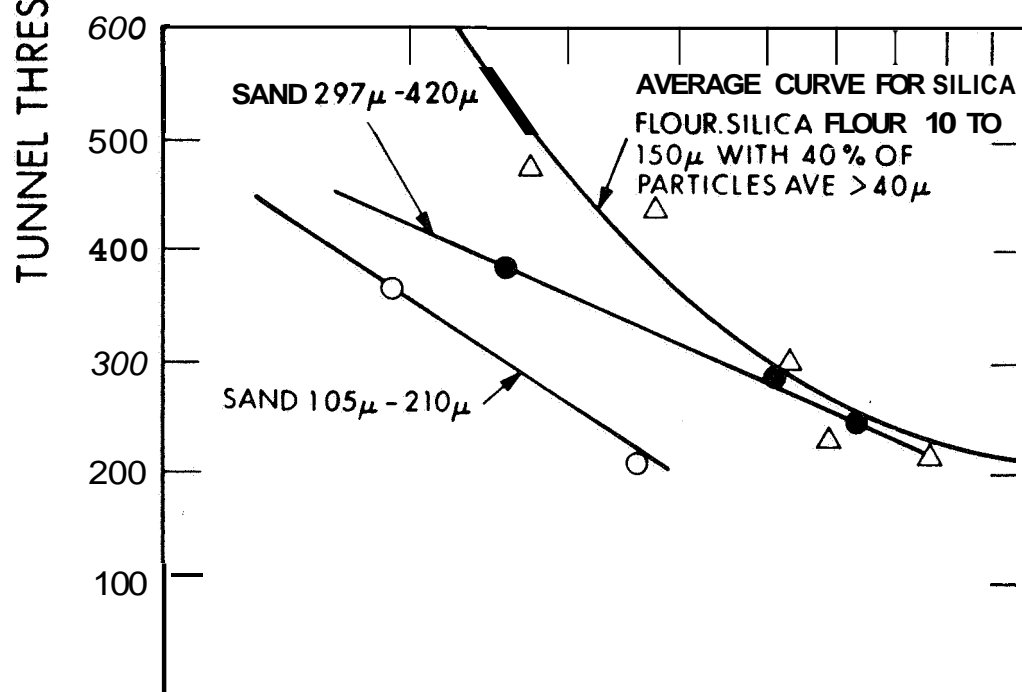
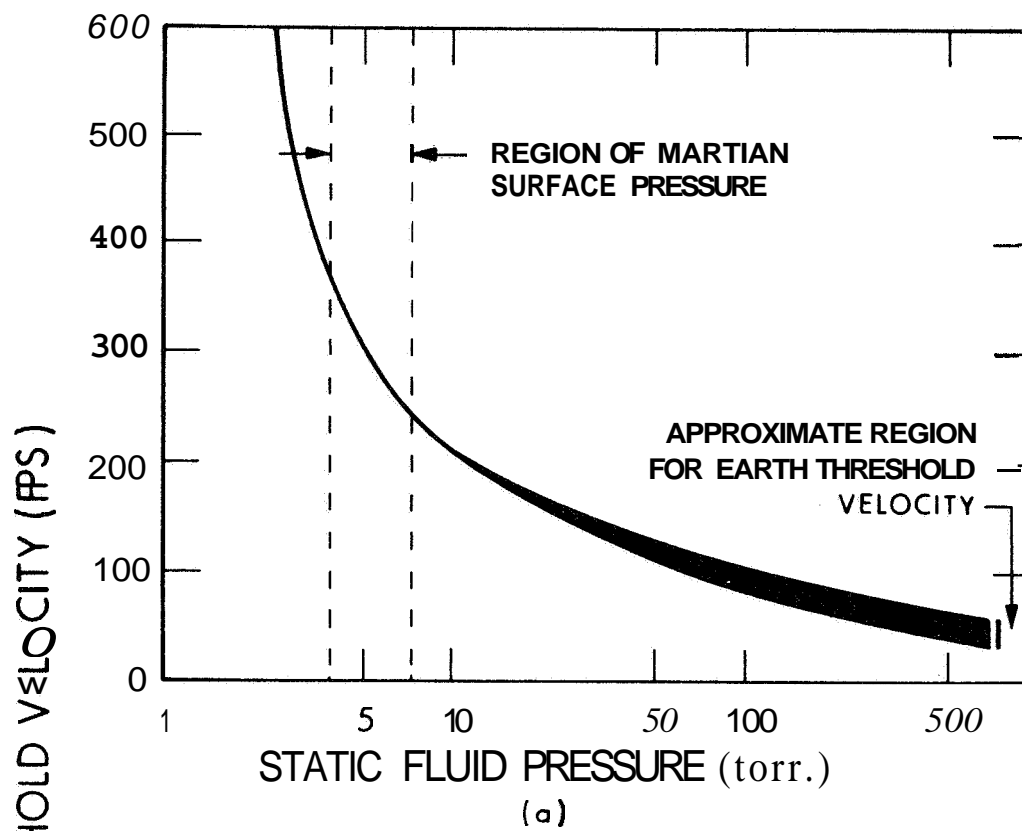
A recent experiment by Hertzler, et al<sup>\*</sup>, indicated that under normal wind speed conditions, surface abrasion will not occur. However, under gust conditions where wind speed is approximately 400 ft/sec, some surface deterioration can be expected. The experiment performed consists of three parts. The first set of experiments was primarily concerned with the deterioration of wind threshold velocity (the speed at which dust particles become airborne). The threshold velocity as a function of the surface pressure and particle size is shown in Fig. 15.

The second set of experiments was concerned with the determination of the particle concentration at various speeds, ranging from 344 to 435 ft/sec. The particle size ranged from 10 to 420 $\mu$ . Results indicated that the particle concentration varied from  $10^{-4}$  to  $10^{-5}$  oz/ft<sup>3</sup> of flow.

The third set was the abrasion experiment, where surface deterioration of various coatings was determined at several combinations of particle concentrations, wind speeds, and surface pressure. Results of this experiment where the specimen surface was normal to the wind velocity

---

<sup>\*</sup>"Martian Sand and Dust Storm Experimentation" by Richard G. Hertzler, Emile J. J. Wang, and Ollie J. Wilbers, J. Spacecraft, Vol. 4, No. 2, p. 284-286.



are shown in Table VIII. It can be seen that the damage to the glass surface varied from local pitting at 300 ft/sec to frosted conditions at 520 ft/sec. The damage to thermal control coating varied from local abrasion to complete coating removal.

Based on these results the following conclusions can be drawn:

- a. Although this experiment was preliminary, results indicated the problem could be serious.
- b. More experimentation should be performed to confirm reproducibility, perhaps by another independent source.
- c. The experiment should take into consideration that the Martian gravitational field is 0.38 that of Earth's. This could result in a higher dust particle concentration than what was reported for the same wind speed and pressure.
- d. The experiment should be directed towards a more closely simulated condition of Mars probable model, especially in the regime of 380 to 450 ft/sec wind and 5 to 7 mb surface pressure.
- e. The surface specimen should be tested at various angles with respect to wind direction. Perhaps the simplest solution will be to employ sensors which control the panel orientation in such a way as to minimize the damage. In fact, the wind load on panels during storm conditions may be simultaneously reduced in this manner.

TABLE VIII

## RESULTS OF ABRASION EXPERIMENTS

Specimen		Abrasion material <sup>b</sup>	Particle conc., <sup>c</sup> oz/ft <sup>3</sup>	Abrasion Conditions				Results
Substrate	Coating <sup>a</sup>			Velocity, fps	Pressure, torr	Pressure, mb	Duration, min	
2024 Al	Velvet	Sand	$1.27 \times 10^{-4}$	520	31	4.1	26	Coatings removed
2024 Al	ZnO							
2024 Al Glass	Velvet None	Sand	$1.6 \times 10^{-5}$	300	0.4	5.8	60	Local abrasion Pitting
2024 Al Glass	Velvet None	Flour	$1.03 \times 10^{-5}$	520	4.1	5.4	60	Coating removed Frosted
2024 Al Glass	Velvet None	Flour	$4.03 \times 10^{-5}$	300	38	5.0	90	Local abrasion Pitting

<sup>a</sup> Velvet is 3M Black Velvet, 1 mil thick; ZnO is 4 mils.

<sup>b</sup> See Fig 15 for characterization of sand and silica flour

## SECTION 4

### CONCLUSIONS

In summary, this report concludes the Task I effort, and establishes a baseline of the environmental conditions that will be used in the design.

A preliminary review of the conceptual definitions under Task II has been presented in this report, and will be concluded in the November 15 monthly report. The outline of this effort will be as follows:

- a. Geometric study to obtain the minimum necessary projected array area,
- b. Analysis of the array power profile by orientation types, as a function of latitude, hour, topography, and spacecraft attitude.
- c. Interaction between the array concepts and the spacecraft and/or antenna.
- d. A study of existing developmental solar array panel substrates, and their adaptability into the baseline definitions, for the Martian solar array.
- e. A selection and comparison of at least three array configurations for detailed study under Task III of this contract.